Natural Hazards
and Earth System
Sciences

Open Access

Discussions

EGU

NHESSD

Interactive
comment

Interactive comment on "Hazard Assessment Comparison of Tazhiping Landslide Before and After Treatment" *by* Dong Huang et al.

Dong Huang et al.

dhuang@imde.ac.cn

Received and published: 28 June 2017

Response to Reviewer Comments

Manuscript title: (the original title: Hazard Assessment Comparison of Tazhiping Landslide Before and After Treatment) Manuscript number: 2016-391 Thanks very much for reviewer's comments, which helped us to improve the quality of manuscript. We have made major revisions to address the comments raised by the reviewer. The following responses have been prepared to address reviewer' s comments in a point-by-point fashion. All changes have been marked with RED in the revised manuscript. We would be happy to make further modifications if required. We hope the changes listed have made the manuscript suitable for publication, and we look forward to your response.

General comments

Q1: The paper by Huang et al. addresses relevant scientific and technical questions. It presents a concept and adoption of a well-known method to simulate mass movement processes. The used methods are in principle up to international standards but there is some doubt whether they used the appropriate method for this study.

A1: We acknowledge the remark of the reviewer. This paper addresses an interesting and relevant scientific topic. We adopted a well-known method to simulate mass movement processes. The methods are up to international standards. We are expanding the method in this contribution.

Q2: The scientific methods and assumptions used are valid and outlined clearly. There is some confusion about the mass movement process that is discussed and approached by the presented and adopted rheological model. In principle, the numerical approach in RAMMS can also be used for the simulation of landslides. But it is actually not intended for it and does not take into account specific properties of this kind of mass movement (landslides).

A2: We totally agree with the reviewer. The geomorphic heterogeneity of rapid shallow flow-type landslides such as hillslope debris flows is larger than those observed in channelized debris flows; however, many of these flows can be successfully modeled using the Voellmy-fluid friction relation with a block release initiating the flow (Christen et al., 2012). Therefore, the numerical approach in RAMMS can be used for simulation of flow-type landslides. We have added new interpretation in the new version of the manuscript. Please see Page 2, line 63-64 and the discussion section in the new version of the manuscript.

Q3: The results of the study are not really surprising. Interpretation of the simulation results is derived poorly. Some important questions remain still unanswered, namely the sensitivity of the friction parameters and more important the derivation of the best-fit parameters presented in Table 2. This aspect should be at least considered in the

discussion and ideally in the methods section. While the methods section is very detailed (and also well written in good English) regarding the numeric, no information is given about the modeling procedure and interpretation of the simulation results.

A3: The result of the study is in agreement with field survey results. The derivation of the best-fit parameters is an important issue, which we have elaborated on in the discussion and methodology sections. The present estimation of model parameters can be acquired by laboratory or small-scale experiments in some instances, however calculation of the Voellmy rheological model friction coefficient is difficult. Therefore, we tested different coulomb friction coefficient values ranging between and viscous friction coefficient values ranging between . Finally, we selected the coulomb friction coefficient and viscous friction coefficient in accordance with back-analyses of well-documented landslides (Cepeda, J., et al. 2010; Du et al., 2015). The methods and discussion sections have been revised in the new version of the manuscript. Thank for your compliment on the writing of methods section in the new version of the manuscript. Please see p.12-13, line 271-278 and p.22-23, line 384-411.

Q4: The title does not promise detailed information about the numeric but rather a specification about the hazard assessment comparison. Therefore or the title or the content of the paper should be changed. The same is true for the abstract. More information should be given for the methods section or the method section should be adjusted. The mathematical formulae, symbols, abbreviations and units are correctly defined and used.

A4: Thank you for the insightful comments. We totally agree that the title should be revised. The title of this paper has been revised to "Hazard Assessment Comparison of Tazhiping Landslide Before and After Treatment Using the Finite Volume Method". The corresponding abstract has been revised as well. The methods section has been revised. Please see the response to comment A3. Please see p.1, line 2 and line 12-13; p.12-13, line 271-278.

Q5: There is some confusion in terminology for figures 6 and 7, that have to be changed. Figures should be improved. Figure 1 seems to be taken from an existing paper without citation. Figure 2 needs more information about the location of the study site in a global perspective and better visualization of the exact location in the Baisha river basin. figures 6 and 7 do not contain more details on the landslide area, location of the objects at risk, etc. This information is only given in figure 8 but visualized rather small. Readability of the outlines of buildings is very hard and not mentioned in the legend. The authors give in principle proper credit to previous and related work. Own contributions are not well indicated (besides the adoption of the model and the interpretation of the simulation results).

A5: Thank you for pointing out the accurate terminology. The confusion in terminology for Figures 6 and 7 has been revised. Please see p.14, line 282 and 284; p.16, line 323 and p.17, line 325. We have re-organized and added more information about the location of the study area. The Baisha river basin is visible in Figure 2. Please see p.9, line 214-215. In Figures 6 and 7 we added more detail on the landslide area shown in Figures 7a and 9a. Please see p.13, line 281; and p.16, 322. Figure 10 has been extensively revised. Building outline were added to the legend. Please see p.21, line 376 and p.22, line 379. Various minor modifications and revisions were made to all Figures. Please see p.10, line 216-217 and 218-219.

Q6: Number and quality of the references are appropriate. There are some publications in Chinese that are not accessible by all fellow scientist. There is some confusion for the article by Zhang,Z.Y., Wang,S.T., Wang,L.S.,et al., about the year of publication. In the text 1994 is mentioned while in the references there is written 1993. The reference of Toro, 1992 is missing.

A6: We have deleted some parts of unimportant Chinese's literature and revised all references according to the NHESSD journal style. We have cited the reference of Toro, 1992. Please see references section in the new version of the manuscript. Please see p.2, line 46, 51 and 52.

Q7: Structure and length of the paper is adequate. Methods section with the numeric is too long compared to the results section.

A7: We appreciate the comments. The methods section is very detailed; no more information is given on the simulation results. Thus, we have added more interpretation into the results section. Please see the results section in the new version of the manuscript.

Q8: Technical language and the English is more or less of good quality and understandable. Several sentences need to be reformulated, mostly because of wrong word order. There is no supplementary material available.

A8: We have carefully proofread the whole manuscript to exclude language issues as much as possible. All changes have been marked with BULE in the revised manuscript.

Other specific comments are given below.

Q9: p.2, line 61: what do the authors exactly mean with "landslide-debris flows?" Please rely on some definitions in the literature.

A9: Landslides move downslope in many different ways (Varnes, 1978). Flow-type landslides can evolve into rapidly travelling flows, which exhibit characteristics of debris flows on unchannelized or only weakly channelized hillslopes. The geomorphic heterogeneity of rapid shallow flow-type landslides such as hillslope debris flows is larger than those observed in channelized debris flows, however, many of these flows can be successfully modelled using the Voellmy-fluid friction relation and with an initial block release (Christen et al., 2012). It is true that there is some confusion about the term "landslide-debris flows" used here. We have revised it to "flow-type landslides" and add some definitions from the literature. Please see p2, line 63-64 and discussion section p22 and 23.

Q10: p.2, line 71: what to the authors exactly mean with 3D mapping of the division of hazard zones? Usually, hazards zonation is given on a map, e.g. in 2D

A10: Thank you for the correction. It has been revised to 2D. Please see p.2, line 74.

Q11: p.3, line 98: this figure is taken from Christen et al., 2010. Please cite source.

A11:It has been added. Please see p.3, line 101.

Q12: p.3, line 107: missing space.

A12: It has been revised. Please see p.4, line 109.

Q13: p.7, line 178: this reference is missing in the reference section.

A13: It has been cited. Please see reference p.26, line 539-540 and p.7, line 178 -179. " Toro, E.F.: Riemann problems and the waf method for solving the two dimensional shallow water equations, Philos. Trans. R. Soc. London, Ser., A 338, 43–68. 1992".

Q14: p.11, line 255: see comment for p.2, line 71

A14: It has been revised to 2D. Please see p.12, line 263.

Q15: p.11, line 266: figure is subtitled with "Thickness". Thickness of deposition is not equal to flow height (if a landslide really "flows"...). Please adapt wording.

A15: Thank you for pointing out the inaccurate terminology. It has been revised to flow height. Please see p.1, line 15; see p.14, line 282; p15, line 292 and 294; p.16, line 323; p17, line 332 and 334; p18, line341; p23, line 416.

Q16: p.12, line 268: subtitle of figure is "Speed", legend says "Velocity". If the blue to green marked zone shows the deposited mass of the landslide, there should be no velocity value (because it's deposited). In chapter 3 is no indication or estimation about the speed of the landslide mass, therefore figure 6b does not really make sense.

A16: Thank you for pointing out the inaccurate terminology. It has been revised to Velocity. Please see p.1, line 15; p.14, line 284; p15, line 295 and p.17, line 325 and 334. In any case, velocity plays a more important role regarding kinetic energy acting on an obstacle. However, the Miaoba residential area of Red Village is located at the frontal part of Tazhiping landslide. Therefore, the maximum flow height of the landslide

is one of the direct factors influencing the building's deformation failure status. Please see p.18, line 346-353.

Q17: p.12, line 270: not clear, if the colored area shows the maximum pressure or an instantaneous for a given time step. Much more of interest would be a local value (over time) at the position of a building. And why the legend goes up to more than 1000kPa but no reddih or yellowish areas are marked?

A17: The colored area shows the maximum values of moving process or an instantaneous pressure for a given time step. As the building of Red Village is located at the frontal part of landslide, the pressure of the middle and lower landslide deposits was about 200kPa. Thus, three-story and lower houses within the deposition range might be buried. The maximum pressure value in the surface gully can be found in the middle and upper slope. According to field surveys, we have found this gully is at an elevation of about 1,200 m. The maximum pressure value is easily found from the instantaneous for a given time step figure. Therefore, coupled with field observations and numerical simulation, they are especially helpful in understanding the landslide movement process in complex terrain. It has been introduced in p.17, line 329-330.

Q18: p.12, lines 274, 277 and p.13, line 278: not clear what numbers in the circle mean. Is this kind of a list or does it indicate a location in a figure?

A18: No, it does not indicate a location. It has been deleted. Please see p.14, line 291; p.15, line 294 and 295.

Q19: p.13, line 279: how is made this separation between houses of different numbers of stories? Please give more information and references to it.

A19: The building is 3m high on each floor. We have cited some literature (Hungr et al., 1984; Petrazzuoli et al., 2004; GB, 50010–2010; Hu et al., 2012; Zeng et al., 2015). Please see p18, line 362 and 364.

Q20: p.13, line 293: or indicate "about 1.2 m" or give exact value.

A20: The more exact value has been given. " with an elevation of 1,070-1,072m and a length of 182m." Please see p.15, line 317-318.

Q21: p.13, line 298: same remark as for figure 6a.

A21: It has been revised. Please see A.15.

Q22: p. 14, line 300: same remark as for figure 6b

A22: It has been revised. Please see A.16.

Q23: p.14, line 305: example of a sentence that has to be rewritten because of wrong word order.

A23: We have revised the sentence to read "Provided in Fig.9 are the kinematic characteristics of the landslide deposit." Please see p.17, line 329.

Q24: p.14, lines 305, 308, 309: not clear what numbers in the circle mean.

A24: It has been deleted. Please see p.17, line 331 and 334; p.18, line 335.

Q25: p.15, line 321/322: not sure, if this statement is really true. There may be examples where entire houses on a landslide mass are moved but not destroyed because of stable base plates. In any case, velocity plays a more important role regarding kinetic energy acting on an obstacle. You are right in the sense that the height of a moving landslide (e.g. the frontal part) plays an important role when it hits a building on a higher level, e.g. the second or third floor. Please clarify this point.

A25: We have clarified this point. "Landslides reflect landscape instability that evolves over meteorological and geological timescales, and they also pose threats to people, property, and the environment. The severity of these threats depends largely on landslide speed and travel distance. There may be examples where entire houses on a landslide mass are moved but not destroyed because of stable base plates. In any case, velocity plays a more important role regarding kinetic energy acting on an obstacle. However, the Miaoba residential area of Red Village is located at the frontal part

of Tazhiping landslide." Please see p.18, lines 346-353.

Q26: p.15, 16 and 17, table 3: the term "washed away" is not suitable for landslide process. It implies an major influence by a fluid.

A26: It has been revised. Please see p.18, line 366.

Q27: p.17, line 333: This should be 2D, because you show a map with the different zonations. These different zonations are not defined, by the way.

A27: It has been revised to 2D. Please see p.20, line 367 and p.22, line 381.

Q28: p.17, line 339: There seem to be marked buildings (in the red high-hazard zone). If so, adjust legend and make sure they are better visible. What zone is defined outside the colored area? No hazard or also low-hazard zone?

A28: In figure 10, the red high-hazard zone of buildings has been marded. We have adjusted the legend and defined outside the colored area as no-hazard. Please see p.20, line 371-374 and Figure.10 legend.

Q29: p.18, line 342: same as for figure 8a. And this should be 8b instead of 8c.

A29: It has been revised. Please see p.22, line 381.

Q30: p.18, line 350: what is a landslide-debris flow?

A30: It has been defined. Please see p.23, line 389-396 and answer A5.

Q31: p.18, line 358: this should be 2D.

A31: It has been revised. Please see p.23, line 423.

Q32: p.19, line 411: correct reference would be: Michael-Leiba, M., Baynes, F" Scott, G., Granger, K. 2003. Regional landslide risk to the Cairns community [J]. NatHazards, 2003,30 (2):233–249. Check reference style for all references according to the journal style!

A32: We have revised all references according to the NHESSD journal style. The reference list has been updated as well. Please see references section.

The text of the manuscript has been revised.

Please also note the supplement to this comment:
https://www.nat-hazards-earth-syst-sci-discuss.net/nhess-2016-391/nhess-2016-391-AC7-supplement.pdf

Interactive comment on Nat. Hazards Earth Syst. Sci. Discuss., https://doi.org/10.5194/nhess-2016-391, 2017.

Hazard Assessment Comparison of Tazhiping Landslide Before and After Treatment using the finite volume method

Dong Huang [1], YuanJun Jiang[1]*, JianPing Qiao[1], Meng Wang[1]

1. Key Laboratory of Mountain hazards and Surface process, Institute of Mountain hazards and Environment, Chinese Academy of Science, Chengdu 610041, China
*Corresponding author (yuanjun.jiang.civil@gmail.com).

Abstract: Through investigation and analysis of geological conditions and mechanical parameters of the Taziping landslide, the finite volume method was adopted, and, the rheological model was adopted to simulate the landslide and avalanche entire mass movement process. The present paper adopted the numerical approach of RAMMS and the GIS platform to simulate the mass movement process before and after treatment. This paper also provided the conditions and characteristic parameters of soil deposits (thickness flow height, speed velocity, and stresses) during the landslide mass movement process and mapped the 3D division of hazard zones before and after landslide treatment. Results indicated that the scope of hazard zones contracted after engineering treatment of the landslide. The extent of high-hazard zones was reduced by about 2/3 of the area before treatment, and characteristic parameters of the mass movement process after treatment decreased to 1/3 of those before treatment. Despite engineering treatment, the Taziping landslide still poses significant hazard to nearby settlements. Therefore, we propose that houses located in high-hazard zones be relocated or reinforced for protection.

Keywords: finite volume method; rheological model; motion feature parameters; hazard assessment

1. Introduction

The hazards of a landslide include scope of influence (i.e., source area, possible path area, and backward and lateral expansion area) and secondary disasters (i.e., reservoir surge, blast, and landslide-induced barrier lake). A typical landslide hazard assessment aims to propose a systematic hazard assessment method with regard to a given position or a potential landslide. Current research on typical landslide hazard assessment remains immature, and there are multiple methods for interpreting landslide hazards. To be specific, the scope of influence prediction of a landslide refers to deformation and instability characteristics such as sliding distance, movement speed, and bulking thickness range. The movement behavior of a landslide mass is related to its occurrence, sliding mechanisms, mass characteristics, sliding path, and many other factors. Current landslide movement prediction methods include empirical prediction and numerical simulation.

Empirical prediction method: The empirical prediction method involves

analyzing landslide flow through the collection of landslide parameters in the field. It further consists of the geomorphologic method (Costa, 1984; Jackson et al., 1987; Scott et al., 1993), the geometric change method (Zhang et al., 1994 1993; Finlay et al., 1999; Michael-Leiba et al., 2003), and the volume change method (Fannin et al., 2001). Empirical models are commonly simple and easy to apply, and the required data are easy to obtain as well. **Numerical simulation method:** Numerical simulation methods are further divided into the continuous deformation analysis method (Hungr, 1995; Evans et al., 2009; Zhang .Y, 2013; Wang. L, et al., 2016), the discontinuous deformation analysis method (Shi.G.H, 1988; Yin et al., 2002), and the simplified analytical simulation method (Christen et al., 2010a; Sassa, 2010; Bartelt et al., 2012; Du et al., 2015). The numerical simulation method expresses continuous physical variables using the original spatial and temporal coordinates with geometric values of discrete points. Numerical simulations follow certain rules to establish an algebraic equation set in order to obtain approximate solutions for physical variables.

Empirical prediction models only provide a simple prediction of the sliding path. Due to the differences in geological environments, empirical prediction models commonly have low generality. The continuous deformation method has the advantage of an extremely strong replication capability, but it is not recommended when analyzing flow-type landslides debris flows, lahars, or debris flows because of complicated rheological behaviors (Iverson et al., 1997, 2001; Hungr et al., 2001; Glade 2005; Portilla et al., 2010; Chen et al., 2014). The fluid mechanics-based discontinuous deformation method has several shortcomings such as, great computational burden, difficult parameter selection, and difficult 3D implementation. The simplified analytical simulation method fully takes into account the flow state properties of landslides before introducing a rheological model and can easily realize 3D implementation on the GIS platform. On that account, this paper adopted the continuous fluid mechanics-based finite volume method (simplified analytical simulation method). We introduce a rheological model on the basis of using mass as well as momentum and energy conservation to describe the movement of landslides. We also employed GIS analysis to simulate the entire movement process of Taziping landslide and map the 32D division of hazard zones.

2. Methods

2.1 Kinetic analysis method

Adopting the continuous fluid mechanics-based finite volume method, this paper took into account erosion action on the lower surface of the sliding mass and the change in frictional resistance within the landslide-debris flow in order to establish a computational model. The basic idea is to divide the calculation area into a series of non-repetitive control volumes, ensuring that there is a control volume around each grid point. Each control volume is then integrated by the unresolved differential equation in order to obtain a set of discrete equations. The unknown variable is the numerical value of the dependent variable at each grid point. To solve the integral of a control volume, we make a hypothesis about the change rule of values among grid

[a4]: Answer to the comment Q6: We have deleted some parts of unimportant Chinese's literature and revised all references according to the NHESSD journal style.

[a5]: Answer to the comment Q6 and Q32: We have deleted some parts of unimportant Chinese's literature and revised all references according to the NHESSD journal style.
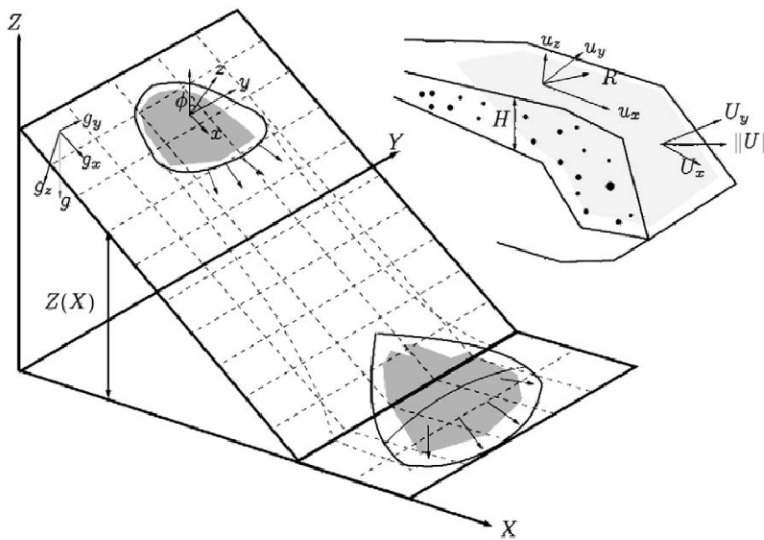
[a6]: Answer to the comment Q6 and Q32: We have deleted some parts of unimportant Chinese's literature and revised all references according to the NHESSD journal style.

[a7]: Answer to the comment Q9: It is true that there is some confusion about the term "landslide-debris flows" we used here. We have revised it to "flow-type landslides".

[a8]: Answer to the comment Q2 and Q9: We have added some definitions in the literature. The more detailed definition in the discussion part.

[a9]: Answer to the comment Q10: It has been revised to 2D.

87 points, that is, about their piecewise distribution profile. The finite volume method
88 can satisfactorily overcome the finite element method's weakness of slow calculation,
89 and solve the problem of complex region processing. Thus, we adopted the finite
90 volume method to establish the kinematic model for the landslide flow process.
91   The core of the finite volume method is domain discretization. The finite volume
92 method uses discrete points as a substitute for continuous space. The physical
93 meaning of the discrete equation is the conservation of the dependent variable in a
94 finite control volume. Establishment of the conservation equation is based on the
95 continuous movement model, that is, the continuity hypothesis about landslide
96 substances. We divided the landslide mass into a series of units and made the
97 hypothesis that each unit has consistent kinematic parameters (speed at a depth,
98 density, etc.) and physical parameters (Fig.1). We also established an Eulerian
99 coordinate system-based conservation equation with regard to each control volume.

100

101   Fig.1 Schematic diagram of finite volume discretization (Christen et al., 2010a).

102 **2.2 Control equation**

103   The computational domain is defined as directions x and y, and the

104 topographic elevation is given the coordinate $z(x, y)$. $H(x, y, t)$ is assumed as the

105 change relationship of landslide thickness with time; $U_x(x, y, t)$ and $U_y(x, y, t)$

106 respectively represent the mean movement speeds along directions x and y at

107 moment t; $n_x = U_x \big/ \sqrt{U_x^2 + U_y^2}$ and $n_y = U_y \big/ \sqrt{U_x^2 + U_y^2}$ represent the cosinoidal and

108 sinusoidal flow vectors of the landslide on the plane x-y. The mean flow speed of

109

3

109 substances is defined as $U = \sqrt{U_x^2 + U_y^2}$.

110   Thus, the mass balance equation becomes:

111
$$\partial_t H + \partial_x (HU_x) + \partial_y (HU_y) = \dot{Q} \tag{1}$$

112   wherein, $\dot{Q}(x,y,t)$ represents the change rate (entrainment rate) of landslide

113 volume with time.

114   Assuming that $l(x,y,t)$ represents the movement distance of the landslide with

115 time, we can obtain:

116
$$\dot{Q} = \begin{cases} 0 & if & h_i = 0 \\ \dfrac{\rho_i}{\rho_a} h_i \dfrac{U}{l} & if & k_i l \geq h_i \\ \dfrac{\rho_i}{\rho_a} k_i U & if & k_i l < h_i \end{cases} \tag{2}$$

117   wherein, h_i represents the thickness of the i th layer of the landslide in the

118 movement process; ρ_i represents the density of the i th layer of the landslide in the

119 movement process; ρ_a represents the density of the landslide; the dimensionless

120 parameter k_i represents the entrainment rate.

121   The momentum balance equation is:

122
$$\partial_t (HU_x) + \partial_x (HU_x^2 + \frac{g_z k_{a/p} H^2}{2}) + \partial_y (HU_x U_y) = S_{gy} - S_f (R)[n_x] \tag{3}$$

123
$$\partial_t (HU_y) + \partial_y (HU_y^2 + \frac{g_z k_{a/p} H^2}{2}) + \partial_x (HU_x U_y) = S_{gx} - S_f (R)[n_y] \tag{4}$$

124   wherein, $S_{gx} = g_x H$ and $S_{gy} = g_y H$ represent the dynamic components of the

125 acceleration of gravity in directions x and y ; $g = (g_x \quad g_y \quad g_z)$ represents the

126 vector of the acceleration of gravity; $k_{a/p}$ represents the pressure coefficient of soil;

127 ρ_a represents the density of the landslide; the dimensionless parameter k_i

128 represents the entrainment rate; $S_f (R)$ represents the frictional resistance.

129   The kinetic energy balance equation is:

130
$$\partial_t (HR) + \partial_x (HRU_x) + \partial_y (HRU_y) = \dot{P} - \dot{D} \tag{5}$$

4

131   wherein, $R(x,y,t)$ represents the random mean kinetic energy of the landslide;

132    $\dot{P}(x,y,t)$ and $\dot{D}(x,y,t)$ represent the random increased kinetic energy and decreased

133   kinetic energy of the landslide.

2.3 Constitutive relationship

135   The improved Voellmy rheological model is applied in the computational

136   simulation of the landslide. See the computational formula below:

$$S_f = \frac{u_i}{\|U\|}\left(h\mu g_z + R_t U^2 + R_\zeta U^2\right) \tag{6}$$

$$R_t = \mu h \frac{U^T K U}{U^2}, R_\zeta = \frac{g}{\zeta} \tag{7}$$

139   wherein, $u_i/\|U\|$ represents the unit vector in the movement direction of the

140   landslide; μ represents the Coulomb friction coefficient, and is related to $R(x,y,t)$,

141   the random mean kinetic energy of the landslide; R_t represents the gravity-related

142   frictional force coefficient; K represents the substrate surface curvature; ζ

143   represents the viscous friction coefficient of the "turbulent flow".

2.4 HLLE-Heun numerical solution

145   Synthesizing control equations (1), (3), (4) and (5), we can obtain the simplified

146   form of the nonlinear hyperbola equation:

$$\partial_t V + \nabla \cdot F(V) = G(V) \tag{8}$$

$$V = \begin{pmatrix} H \\ HU_x \\ HU_y \\ HR \end{pmatrix} \qquad G(V) := \begin{pmatrix} \dot{Q} \\ S_{gx} - S_{fx} \\ S_{gy} - S_{fy} \\ \dot{P} - \dot{D} \end{pmatrix}$$

$$F(V) = \begin{pmatrix} HU_x & HU_y \\ HU_x^2 + g_z k_{a/p} \dfrac{H^2}{2} & HU_x U_y \\ HU_x U_y & HU_y^2 + g_z k_{a/p} \dfrac{H^2}{2} \\ HRU_x & HRU_y \end{pmatrix}$$

150   wherein, $V(x,y,t)$ represents a vector equation consisting of four unknown

151   vector variables; $F(V)$ represents the flux function; $G(V)$ represents the source

152   term. Based on the HLLE equation of the finite volume method and the quadrilateral

153   grid, the node layout can adopt the grid center pattern, and the normal flux along one

154   side of the control volume can be represented by the flux at the center of the side. The

5

155 finite volume discretization adopting the control volume as unit is depicted in Fig.1;

156 the Gauss theorem can be followed for the integration of equation (8), wherein C_i

157 represents the unit volume; after converting the volume integral flux function $F(V)$

158 into the curved surface integral, we can obtain:

159
$$\int_{C_i} \partial_t V dx + \iint_{\partial C_i} F(V) \cdot n_i d\sigma = \int_{C_i} G(V) dx \qquad (9)$$

160 wherein, n_i represents the outward normal direction vertical to unit C_i at the

161 boundary; through adopting the HLL format for the discretization of surface integral,
162 the following simplified form can be obtained:

163
$$V_i^{(*)} = V_i^{(n)} + \frac{\Delta t}{A_{C_i}} \Delta F_i^{(HLL)}\left(V^{(n)}\right) \qquad (10)$$

164
$$V_i^{(**)} = V_i^{(*)} + \frac{\Delta t}{A_{C_i}} \Delta F_i^{(HLL)}\left(V^{(*)}\right) \qquad (11)$$

165
$$V_i^{(n+1)} = \frac{1}{2}\left(V_i^{(n)} + V_i^{(**)}\right) \qquad (12)$$

166 wherein, $V_i^{(n)}$ represents the mean value of unit variables at moment $t^{(n)}$; $V^{(n)}$

167 represents the mean value of the entire grid at moment $t^{(n)}$; $\Delta t := t^{(n-1)} - t^{(n)}$ represents

168 the calculated time step; A_{C_i} represents the area of unit C_i; $\Delta F_i^{(HLL)}$ represents the

169 approximate value of the curved surface integral, as shown below:

170
$$\Delta F_i^{(HLL)}\left(V^{(n)}\right) := -\sum_{j=1}^{4} F_{ij}^{(HLL)}\left(V^{(n)}\right) n_{ij} \Delta X \qquad (13)$$

171 wherein, n_{ij} represents the outward normal direction of the i th unit at

172 boundary j; the flux calculation term $F_{ij}^{(HLL)}\left(V^{(n)}\right)$ represents the approximate

173 solution mode of the Riemann problem of the i th unit at boundary j; see the

174 computational formula below:

175
$$F_{ij}^{(HLL)}\left(V^{(n)}\right) = \begin{cases} F\left(V_L^{(n)}\right) & 0 \leq S_L \\ \dfrac{S_R F\left(V_L^{(n)}\right) - S_L F\left(V_R^{(n)}\right) + S_R S_L F\left(V_R^{(n)} - V_L^{(n)}\right)}{S_R - S_L} & S_L \leq 0 \leq S_R \\ F\left(V_R^{(n)}\right) & S_R \leq 0 \end{cases} \qquad (14)$$

176 wherein, $V_L^{(n)}$ and $V_R^{(n)}$ respectively represent the approximate values of $V^{(n)}$

6

177 on both sides of boundary j of the ith unit; S_L and S_R respectively represent the

178 wave speeds on the left and right sides. Refer to the computational method described

179 by Toro (1992). In addition, the gradient magnitude in the original second-order

180 difference equation can be limited through multiplication with the flux limiter, and the

181 second-order format of the TVD property can be constructed to avoid the occurrence

182 of numerical oscillation. Refer to the specific method described by LeVeque (2002).

183   In this paper a numerical solver used within RAMMS is used, which was

184 specifically designed to provide landslide (avalanche) engineers with a tool that can

185 be applied to analyze problems that with two-dimensional depth-averaged mass and

186 momentum equations on three-dimensional terrain using both first and second-order

187 finite volume methods (Christen et al., 2010b).

3. Study area and data

3.1 Taziping landslide

190   The Taziping landslide is located in the southeast of the Hongse Village,

191 Hongkou Town, Dujiangyan City of Sichuan Province. The site is located at

192 (E103°37′46″, N31°6′29″), 68 km away fromwest Chengdu City to the east and 20

193 km away from the Dujiangyan Urban District (Fig. 2). Its geomorphic unit is a

194 middle-mountain tectonic erosional area, falling within the slope geomorphology on

195 the north bank of the Baisha River Valley. As an colluvial layer landslide triggered by

196 the Wenchuan Earthquake,The Taziping Landslide is a large-scale colluvial layer

197 landslide triggered by the Wenchuan Earthquakelandslide as shown in (Fig. 3). It has

198 a gradient of 25°-40° with an average gradient of about 32°. The landslide has an

199 apparent round-backed armchair contour, and has formedwith a steep rear edge,

200 which has a gradient of 35°-50° and an elevation of about 1,370 m. The front edge is

201 located on the south side of the mountain road, and has an elevation of about 1,007 m.

202 The landslide has an elevation difference of about 363 m, and the a main sliding

203 direction of 124°NE. The landslide mass is informs an irregular semi-elliptical shape,

204 and has a length of about 530 m, an average width of 145 m and an landslide area of

205 approximately 7.68×10^4 m^2. The landslide mass is composed of gravelly soil in

206 lithology, and is covered on the surface by silty clay mingled with gravels. In terms of

207 spatial distribution, it the landslide is thick in the middle and thin on the lateral edges,

208 and has a thickness of 20-25 m and a volume of approximately 1.16×10^6 m^3. During

209 the earthquake, the landslide mass slid to cover the northern mountain slope mass of

210 the Hongse Village Miaoba settlement. The landslide has an apparent front edge

211 boundary, and there is also a swelling deformation (Fig. 4).

[a12]: Answer to the comment Q13: It has been cited. Please see reference p.26, line 530-531." Toro, E.F.: Riemann problems and the waf method for solving the two dimensional shallow water equations, Philos. Trans. R. Soc. London, Ser., A 338, 43–68. 1992."
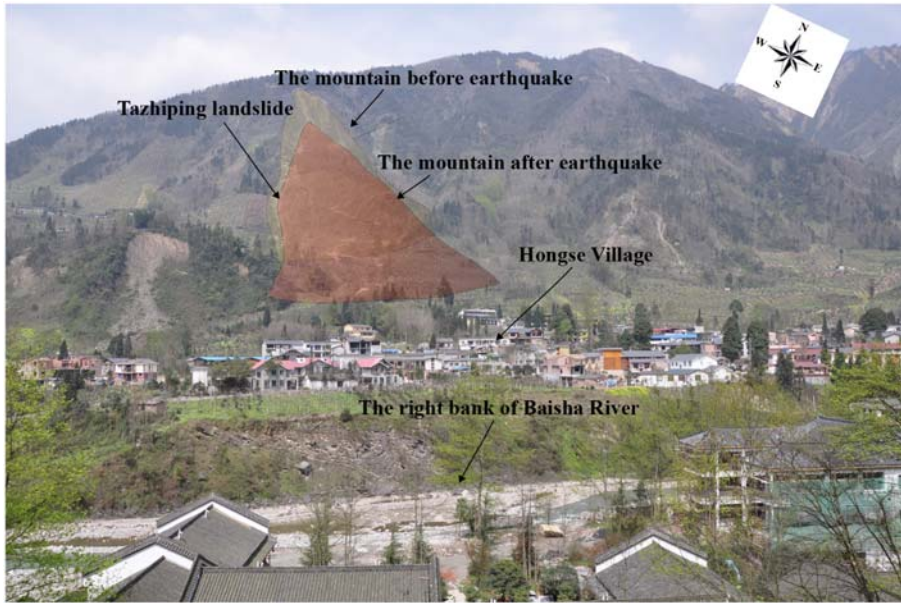
Baisha river basin

Tazhiping landslide

Hongkou town

Hongse village

Baisha river

Baisha river basin in Dujiangyan city

Elevation(m)
High: 4599
Low: 740

0   5,000   10,000
(m)

212

213
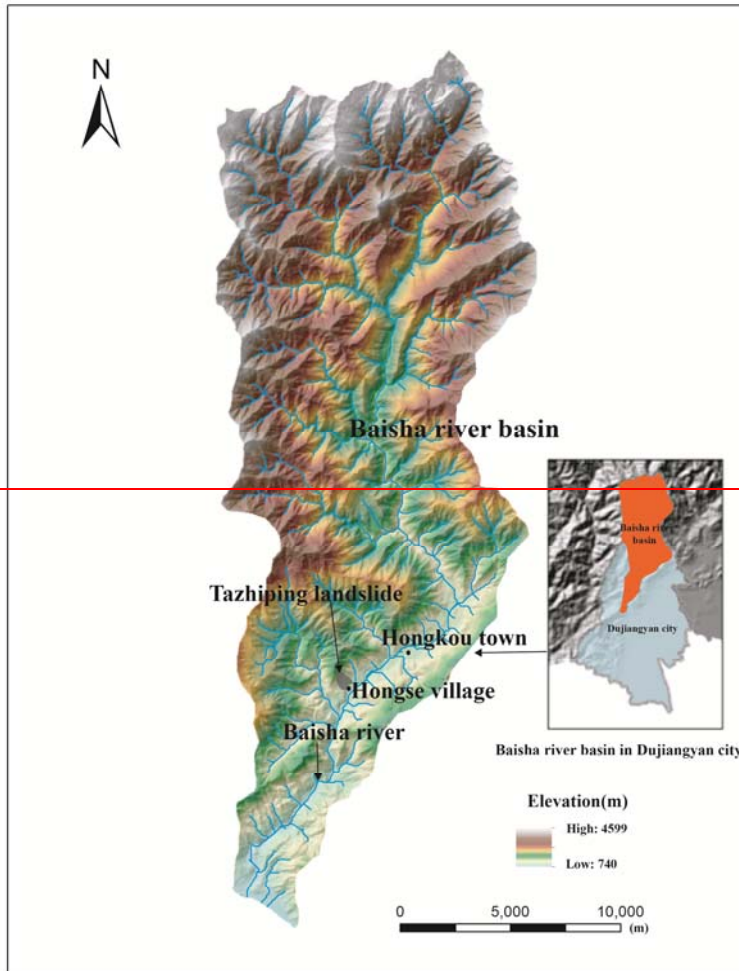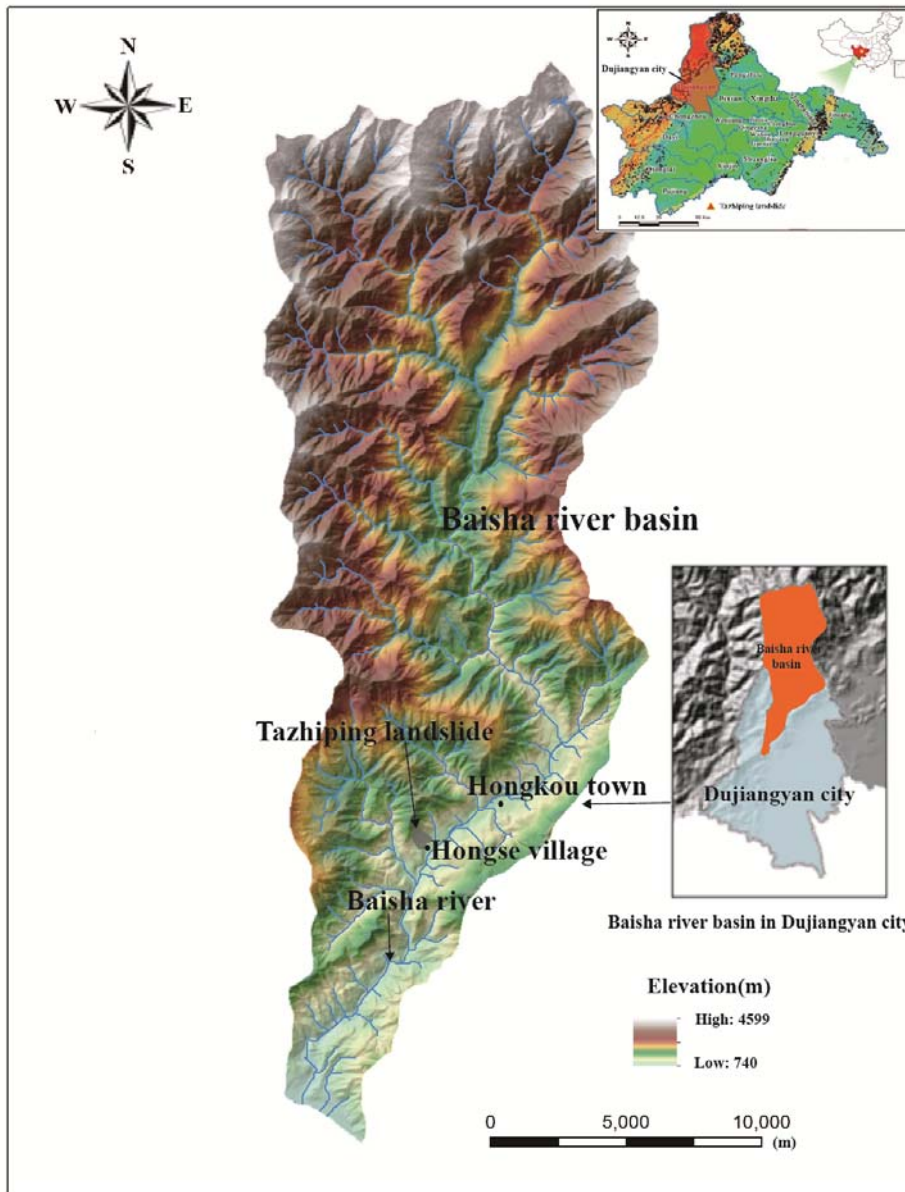
214   Fig.2 Location of Tazhiping landslide, Baisha river basin, Dujiangyan city (the

215   landslide was triggered by Wenchuan Ms 8.0 earthquake on May 12, 2008)

[a13]: Answer to the comment Q5: We have re-organized and added more information about the location of the studying site and Baisha river basin was shown in Figure 2.

216

Fig.3 Taziping Landslide

218

Fig.4 Plane sketch of the Taziping landslide

After the Wenchuan Earthquake, the massive colluvial deposits ~~covers~~ covered ~~on~~ the mountain slope~~, and the landslide mass is dominated by the colluvium~~. The colluvium is ~~mainly distributed on the top surface of the landslide mass in the~~

10

thickness of 0.5-5.0 m ~~thick~~ at the top of the slide, and is ~~mainly constituted by~~composed of rubble~~s~~ and gravel~~s~~. The mass consists of a small amount of fine gravel, ~~substances~~ which ~~are~~ is composed of gray or grayish-green, ~~and dominated by~~ andesite ~~in composition, generally~~ with a ~~block size~~clast of 20-150 cm. Field survey~~s~~ indicate~~s~~ that the rubble~~s~~ in the surface layer ~~have~~ has a maximum diameter exceeding 2 m, and that fine gravel ~~substances are filled among rubbles in a loose structure~~is loosely intercalated with the rubble. ~~Within the thickness of 5-10 m, the landslide mass is constituted of a~~A small amount of yellowish-brown and gray-brown silty clay ~~mingled~~ mixed with 5-40% of non-uniformly distributed ~~broken~~ rubble composed the first 5-10 m of the slide.~~s Within the thickness of~~From 10-25 m deep, there is a wide distribution of gravelly soil. The soil is grayish-green or variegated in color, is slightly compact and non-uniform, and has a ~~broken stone~~rock fragment content of about 50%. The parent rock of the ~~broken stones~~rock fragments is andesite, filled with silty clay or silt (Fig.~~4~~ 5). Table 1 shows the parameters of the surface gravelly soil of the landslide mass based on the field sampling.

<div style="text-align:right">[a16]: We have added Figure4.</div>

Tab.1 Parameters of ~~the~~ surface soil of Taziping Landslide

Internal friction angle (°)		Cohesion (kPa)	Relative compactness	Natural void ratio	Dry density (kN·m⁻³)	Specific gravity (g·cm⁻³)
Peak	Residual					
27.5	23	20.5	53%	0.789	15.357	2.492

slide surface · Q^del colluvial deposit · Q^(dl+el) eluvial deposit · Za proterozoic sinian volcanic group

Fig.~~4~~5 Geological profile of the Taziping Landslide

<div style="text-align:right">[a17]: We have added Figure4.</div>

The landslide is an unconsolidated mass containing relatively large amounts of crushed stones and silty clay (Fig.~~5~~ 6). Its loose structure and strong permeability facilitate infiltration of surface water. The Wenchuan earthquake aggravated the

<div style="text-align:right">[a18]: We have added Figure4.</div>

11

deformation of the landslide making deposits more unconsolidated, further reducing the stability of the landslide mass. During persistent rainfall, surface water infiltrates the landslide slope resulting in increased water pressure within the landslide mass and reduced shear strength on the sliding surface. Thus, rainfall constitutes the primary inducing factor of the upper Taziping landslide. After infiltrating the loose layer, water saturates the slope increasing the dead weight of the sliding mass and reducing the shear strength of soil in the sliding zone. Infiltration into the landslide mass also increases the infiltration pressure of perched water, drives deformation, and poses a great threat to villages located at the front of the landslide. Slide-resistant piles and backfill were place at the toe of the slope in order to reduce the hazards of future slides. The slide-resistant piles have enhanced the overall stability of the slope, however, under heavy rainfall the upper unconsolidated landslide deposits may cut out from the top of the slide-resistant piles.

(a) Material on the landslide surface   (b) Material in the shear zone

Fig.5 6 Photographs showing Colluvial colluvial deposits covers on the mountain slope

Therefore we simulate possible movement states of the Taziping landslide before and after treatment with slide-resistant piles, comparatively analyzed the kinetic parameters in the movement process, and mapped the 3 2D division of hazard zones.

3.2   Hazard prediction before treatment

It was assumed that the landslide was damaged before engineering treatment. According to field investigation, the sliding mass had an estimated starting volume of about 600,000m^3 and a mean thickness of 8m. Based on the survey report and field investigation (Hydrologic Engineering and Geological Survey Institute of Hebei Province, 2010), we adopted the survey parameters of Tab.2 for the simulated calculation. These parameters were obtained from laboratory or small-scale experiments and back-analyses of relatively well-documented landslide cases. The unit weigh $\gamma = 20.8 kN \cdot m^{-3}$ is from small-scale conventional triaxial test experiments in laboratory. In addition, we selected the coulomb friction coefficient $\mu = 0.45$ and viscous friction coefficient $\zeta = 500 m \cdot s^{-2}$ in accordance

12

279

Tab.2 Model calculation parameters

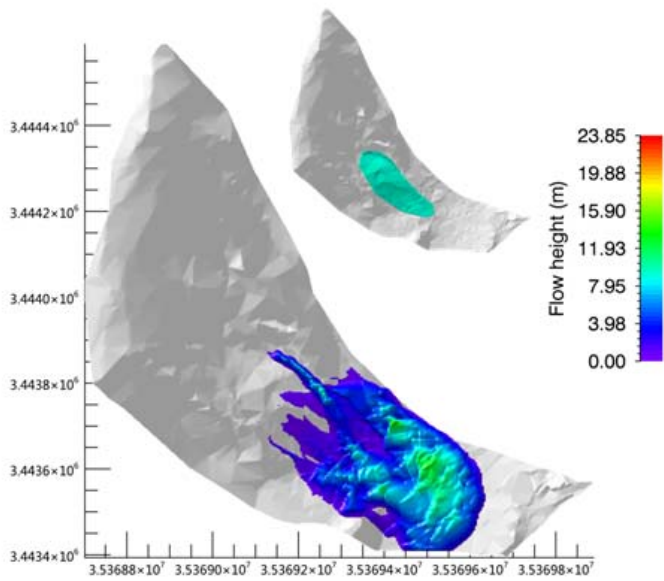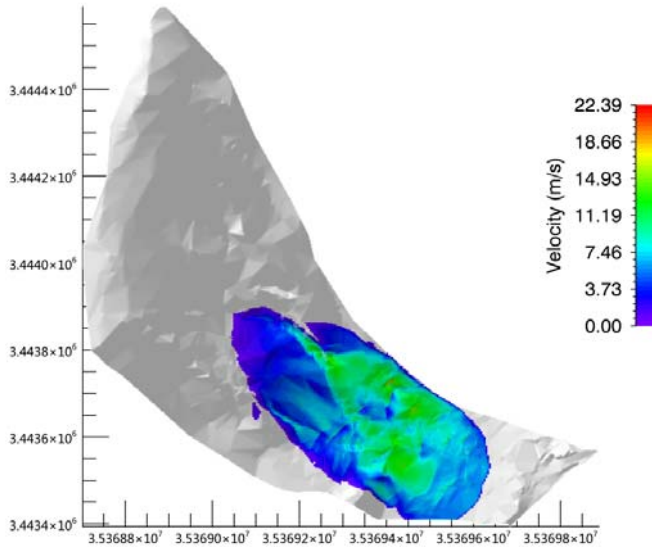| Unit weight $\gamma(kN \cdot m^{-3})$	Coulomb friction coefficient μ	Viscous friction coefficient $\zeta(m \cdot s^{-2})$	Erosional entrainment rate k_i
20.8	0.45	500	0.0001

[a21]: Answer to the comment Q3 and Q4: It is an important issue on the derivation of the best-fit calculated parameters, therefore added more information on the method section.

280

281

13

282   (a) ~~Thickness~~ Flow height

283
284   (b) ~~Speed~~ Velocity

285
286   (c) Pressure

287   Fig. ~~6~~7   Movement characteristic parameters of the Taziping landslide (before

288   treatment)

289   See the kinematic characteristic parameters of the landslide deposits in Fig. ~~6~~ 7.
290 The colored bar shows the maximum values of the kinematic process for a given time
291 step. As shown by the calculation results, ~~①~~ deposits accumulated during the

14

landslide movement process had a maximum ~~thickness~~ flow height of 23.85m, located around the surface gully of the middle and upper slope. The middle and lower section of the landslide deposit~~s~~ had a ~~thickness~~ flow height of about 5-10m; ② the middle and lower movement ~~speed~~ velocity of the landslide ranged from 3m/s and 7m/s; ③ the landslide had a mean pressure of about 500kPa, and the pressure of the middle and lower deposits was about 200kPa. Thus, three-story and lower houses within the deposition range might be buried (The building is 3m high on each floor), and it was further suggested that the design strength of the gable walls of houses on the middle and upper parts of the deposit be increased above 300kPa.

3.3 Hazard prediction after treatment

After fully accounting for the slide-resistant piles and mounds, we introduced the Morgenstern-Price method (Morgenstern et al., 1965) to calculate the stability coefficient of Taziping landslide after treatment. The method was determined with an iterative approach by changing the position of the sliding surface until failure of the dumpsite (Fig.8). The physico-mechanical parameters under a saturated state (Hydrologic Engineering and Geological Survey Institute of Hebei Province, 2010) were adopted to search for the sliding plane of the landslide.

Fig.8 Search for the sliding plane of the Taziping landslide (before treatment)

Based on numerical analysis, the Taziping landslide stability coefficient is 0.998. Under rainfall conditions, the middle area of the Taziping landslide was unstable. Loose deposits in the middle part of the landslide might convert into a high-water landslide ~~substances~~ and cut out from the top of the slide-resistant piles. In the damaged area, the slope had a rear edge wall elevation of about 1,170m. Its front edge was located on the south side of the mountain road, with an elevation of ~~about 1,070m~~ 1,070-1,072m and a length of ~~about 180m~~182m. Thus, the scale of the rainfall-damaged is estimated to be about 250,000m^3, with a mean thickness of about 6m. The parameters in Tab.2 were again adopted for the simulated calculation.

15

[a28]: Answer to the comment Q15: we have revised the terminology.

[a29]: Answer to the comment Q8: We have carefully proofread the whole manuscript to exclude language issues as much as possible.

[a30]: Answer to the comment Q15: we have revised the terminology.

[a31]: Answer to the comment Q18: The numbers in the circle does not indicate a location. It has been deleted.
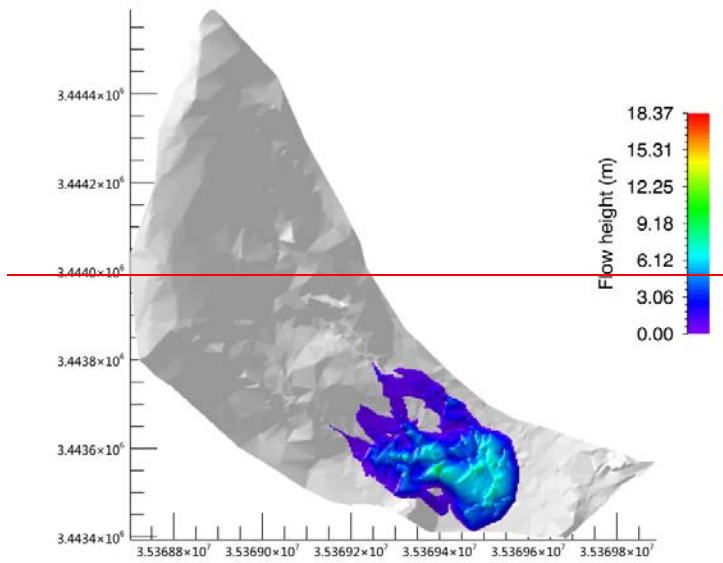
[a32]: Answer to the comment Q16: It has been revised to

[a33]: Answer to the comment Q18: The numbers in the circle does not indicate a location. It has been deleted.
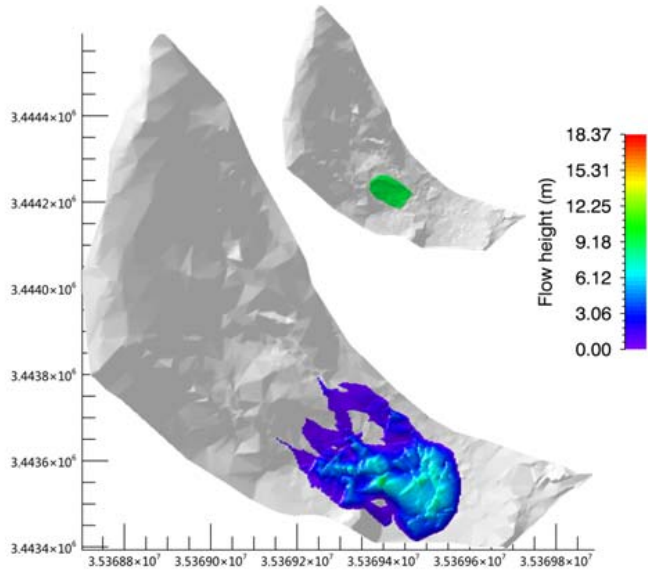
[a34]: Answer to the comment Q19: The building is 3m height each floor.

[a35]: Answer to the comment Q20: The more exact value has been given.
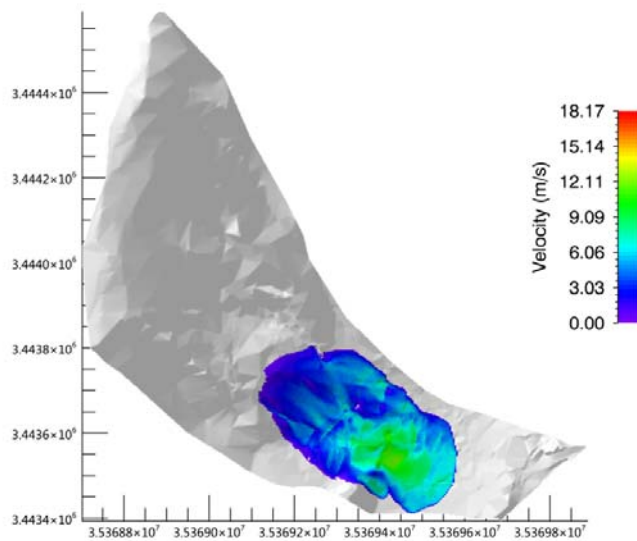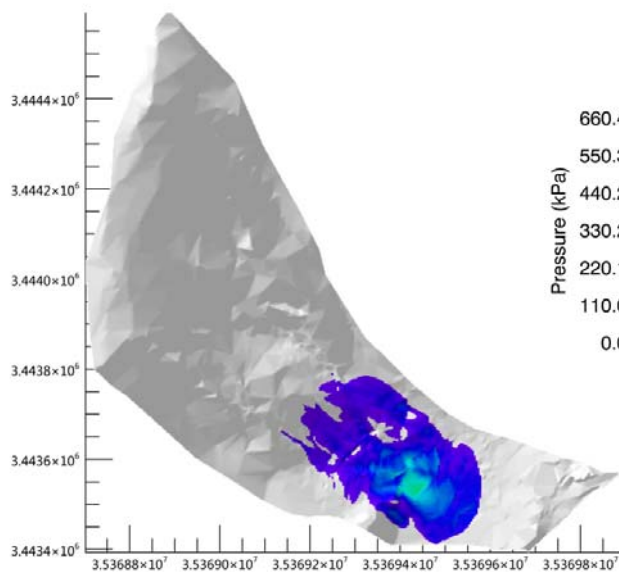
321

322

323   (a) ~~Thickness~~ Flow height

324

325

(b) ~~Speed~~ Velocity

326

327

(c) Pressure

328 Fig. ~~7~~ 9 Movement characteristic parameters of <u>the</u> Taziping landslide (after treatment)

329 Provided in Fig.~~4~~ 9 are the kinematic characteristics of the landslide deposit. The

330 colored bar shows the maximum values of the kinematic process for a given time step.

331 ① Deposits accumulated during the landslide movement process had a maximum

332 ~~thickness~~ flow height of 18.37m, located around the surface gully of the middle and

333 upper slope. The middle and lower portions <u>of the landslide</u> deposit~~s~~ had a ~~thickness~~

334 flow height of approximately 3-5m. ② The middle and lower movement ~~speed~~

velocity of the landslide deposits ranged between 3m/s and 5m/s. ③ The landslide had a mean pressure of about 330kPa, and the pressure of the middle and lower deposits was about 100kPa. Thus, it could be held that two-story and lower houses within the deposition range might be buried. It was further suggested that the design strength of the gable walls of houses on the middle and upper parts of the deposits be increased above 150kPa.

After treatment, the accumulation ~~thickness~~ flow height and pressure of the deposits were reduced by about 1/2, and the kinematic speed ~~was~~ is reduced by about 1/3. However, the Miaoba residential area of Red Village was still partially at hazard.

4 Results

Landslides reflect landscape instability that evolves over meteorological and geological timescales, and they also pose threats to people, property, and the environment. The severity of these threats depends largely on landslide speed and travel distance. There may be examples where entire houses on a landslide mass are moved but not destroyed because of stable base plates. In any case, velocity plays a more important role regarding kinetic energy acting on an obstacle. However, the Miaoba residential area of Red Village is located at the frontal part of Tazhiping lanslide. ~~D~~During landslide movement, the spatial scale indexes of a landslide mass include area, volume, and thickness. The maximum thickness of the landslide is one of the direct factors influencing the building's deformation failure status. A large landslide displacement may lead to burial, collapse, or deformation failure of the building, and thus influence its safety and stability. Thus, landslide thickness constitutes an important index for assessing the hazards of a landslide disaster, and for influencing the consequences faced by disaster-affected bodies (Fell et al., 2008; DZ/T, 0286-2015). Provided in Tab.3 is a landslide thickness-based division of the predicted hazard zones of Taziping landslide, in which the thickness of the landslide mass correlates with the ability of a building to withstand a landslide disaster (Hungr et al., 1984; Petrazzuoli et al., 2004; Glade 2006; GB, 50010–2010; Hu et al., 2012; Zeng et al., 2015). After treatment with slide-resistant piles, the hazard of a future slide was reduced by about 1/3 overall and by 2/3 in high-hazard zones.

Tab.3 Division table of the predicted hazards of Taziping landslide (unit: m^2)

Hazard zone level	Assessment index	Building damage probability	Area before treatment	Area after treatment	Increased/decreased area	Building damage characteristics
Low-hazard zone (l)	$h \leq 0.5$m	20%	44 , 600	38 , 748	-5,852	One-story houses may be damaged; houses on the

						landslide mass are partially damaged. One-story houses have a very high probability of being ~~washed away~~ damaged; one-story houses on the landslide mass are completely damaged.
Relatively low-hazard zone (II)	0.5 m < h≤1m	50~20%	24,900	26,400	+1,500	
						One-story to three-story houses have a very high probability of being ~~washed away~~ damaged; houses less than three stories on the landslide mass are completely damaged.
Moderate-hazard zone (III)	1m < h≤3m	80~50%	21,980	15,856	-6,124	
						One-story houses may be buried, and two-story to six-story houses have a very high probability of being ~~washed away~~
Relatively high-hazard zone (IV)	3m < h≤5m	100~80%	30,820	19,636	-11,184	

[a51]: Answer to the comment Q26: It has been revised.

[a52]: Answer to the comment Q26: It has been revised.

[a53]: Answer to the comment Q26: It has been revised.

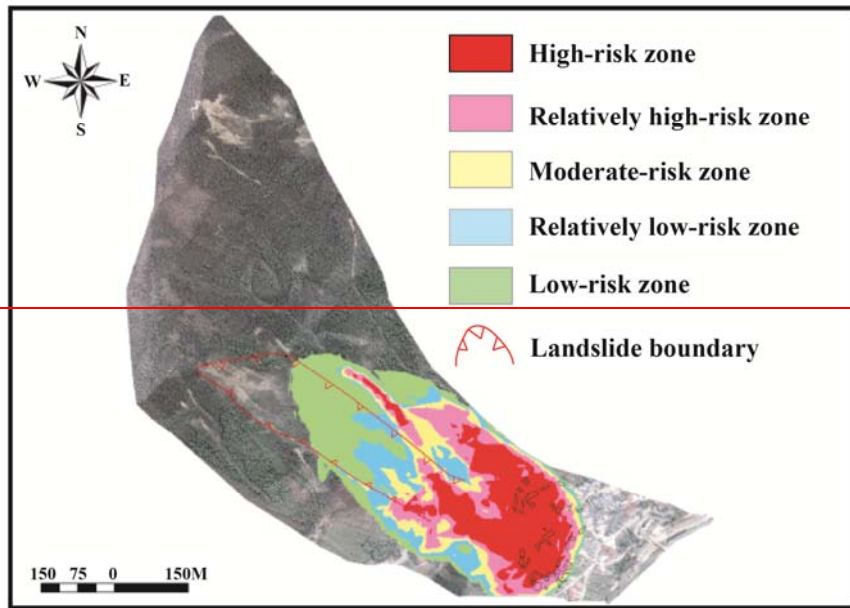|						
High-hazard zone (V)	$h{\geq}5$m	100%	47，240	13，052	-34,188	damaged; houses on the landslide mass are completely damaged. Two-story and lower houses may be buried, and three-story and higher houses have a very high probability of being ~~washed away~~ damaged; houses on the landslide mass are completely damaged.
Total area:	—	—	169，540	113，700	-54,340	—

367 　　Given in Fig.~~8~~ 10 are the ~~3~~2D divisions of hazard zones of <u>the</u> Taziping landslide
368 before and after engineering treatment. The ~~scope~~ <u>size</u> of the hazard zones changed
369 ~~before and~~ after engineering treatment, particularly in the high-hazard zones. Before
370 treatment with slide-resistant piles, the landslide posed a great hazard to eight houses
371 on the left side of the upper Miaoba residential area, with a high-hazard zone
372 associated with landslide mass height over 5m and a red zone. After treatment, the
373 number of effected houses was reduced to four. We defined outside the colored area as
374 no-hazard.

375

376

(a) Before treatment

378

379

380 **(~~e~~b) After treatment**

381 **Fig.~~8~~10 ~~3~~2D division comparison of the hazards of the Taziping landslide**

382

383 **5 Conclusions and Discussion**

384 The hazard assessment of landslides using numerical models is becoming more
385 and more popular as new models are developed and become available for both

22

scientific research and practical applications. There is some confusion about the mass movement process that is discussed by the rheological model presented in this contribution.

Landslides move downslope in many different ways (Varnes, 1978). In addition, landslides can evolve into rapidly travelling flows, which exhibit characteristics of debris flows on unchannelized or only weakly channelized hillslopes. The geomorphic heterogeneity of rapid shallow landslides, such as hillslope debris flows, is larger than observed in channelized debris flows; however many of these flows can be successfully modelled using the Voellmy-fluid friction (Christen et al., 2012). Results presented in this paper support the conclusion that Voellmy-fluid rheological model can be used to simulate flow-type landslides.

The selection of model parameters remains one of the fundamental challenges for numerical calculations of natural hazards. At present, there are numerous empirical parameters obtained from 30-years of monitoring data. Such as in RAMMS, we can automatically generate the friction coefficient of an avalanche for our calculation domain based on topographic data analysis, forest information and global parameters (WSL, 2013). The friction parameters for debris flows can found in some literature (Fannin et al., 2001; Iovine et al., 2003; Hürlimann et al., 2008; Scheidl et al., 2010; Huang et al., 2015). However, there is little research regarding friction parameters of flow-type landslide. Therefore, we tested different coulomb friction coefficient μ values ranging between $0.1 \leq \mu \leq 0.6$ and viscous friction coefficient ζ values ranging between $100 \leq \mu \leq 1000 m \cdot s^{-2}$. Finally, we selected the coulomb friction coefficient $\mu = 0.45$ and viscous friction coefficient $\zeta = 500 m \cdot s^{-2}$ in accordance with back-analyses of well-documented landslides (Cepeda et al., 2010; Du et al., 2015). Simulation results are consistent with field observations of topography and sliding path.

Based on the finite volume method and the RAMMS program, the simulation results of Taziping landslide were consistent with the sliding path predicted by the field investigation. This correlation indicates that numerical simulation is an effective method for studying the movement processes of flow-type landslides debris flows. The accumulation thickness flow height and pressure of landslide deposits were reduced by about 1/2, and the kinematic speed was reduced by about 1/3 after treatment. However, the Miaoba residential area of Red Village is still partially at hazard. Considering that two-story and lower houses within the deposition range might be buried, it was further suggested that the design strength of the gable walls of houses on the middle and upper parts of the deposit be increased above 150kPa.

By utilizing a GIS platform in combination with landslide hazard assessment indexes, we mapped the 32D division of the Taziping landslide hazard zones before and after engineering treatment. The results indicated that overall hazard zones contracted after engineering treatment and, the area of high-hazard zones was reduced by about 2/3. After engineering treatment, the number of at hazard houses on the left

[a63]: Answer to the comment Q3 , Q9 and Q30: The text in the discussion section have been revised. what is a landslide-debris flow? It has been defined.

[a64]: Answer to the comment Q9: It is true that there is some confusion about the term "landslide-debris flows" we used here. We have revised it to "flow-type landslides".

[a65]: Answer to the comment Q15: we have revised the terminology.

[a66]: Answer to the comment Q31: It has been revised to 2D.

23

side of the upper Miaoba residential area, was reduced from eight to four. It was thus clear that some zones are still at high hazard despite engineering treatment. Therefore, it was proposed that houses located in high-hazard zones be relocated or reinforced for protection.

Reference

Bartelt, P., Bühler, Y., Buser, O., Christen, M., and Meier, L.: Modeling massdependent flow regime transitions to predict the stopping and depositional behavior of snow avalanches, J. Geophys. Res., 117, F01015, doi:10.1029/2010JF001957, 2012 .

Costa, J.E.: Physical geomorphology of debris flows. Developments and Applications of Geomorphology, Springer Press., 268-317, 1984.

Christen, M., Kowalski, J., and Bartelt, P.: RAMMS: Numerical simulation of dense snow avalanches in three-dimensional terrain, Cold Regions Science and Technology., 63, 1–14, 2010.

Christen, M., Bartelt, P., and Kowalski, J.: Back calculation of the In den Arelen avalanche with RAMMS: interpretation of model results, Annals of Glaciology., 51, 161–168, 2010.

Christen, M., Bühler, Y., Bartelt, P., Leine, R., Glover, J., Schweizer, A., Graf, C., McArdell, B., Gerber, W., Deubelbeiss, Y., Feistl, T., and Volkwein, A.: Integral hazard management using a unified software environment: numerical simulation tool "RAMMS" for gravitational natural hazards, In: Koboltschnig, G., Hübl, J., Braun, J. (eds.) Proceedings of 12th Congress INTERPRAE., 1, 77–86, 2012.

Chen, J.C., and Chuang, M.R.: Discharge of landslide-induced debris flows: case studies of Typhoon Morakot in southern Taiwan, Nat. Hazards Earth Syst. Sci., 14, 1719-1730, 2014.

Cepeda, J., Chávez, J.A., and Martínez, C.C.: Procedure for the selection of runout model parameters from landslide back-analyses：application to the Metropolitan Area of San Salvador, El Salvador, Landslides., 7, 105–116, 2010.

Du, J., Yin, K.L., and Wang, J.J.: Simulation of three-dimensional movement of landslide-debris flow based on finite volume method, Chinese Journal of Rock Mechanics and Engineering.,

[a67]: Answer to the comment Q32: We have revised all references according to the NHESSD journal style.

470   34: 480–488, 2015 (in Chinese).

471 Evans, S.G., Tutubalina, O.V., Drobyshev, V.N., Chernomorets, S.S., McDougall, S., Petrakov,
472   D.A., and Hungr, O.: Catastrophic detachment and high-velocity long-runout flow of Kolka
473   Glacier, Caucasus Mountains, Russia in 2002, Geomorphology., 105, 314–321, 2009.

474 Fannin, R.J., and Wise, M.P.: An empirical-statistical model for debris flow travel distance,
475   Canadian Geotechnical Journal., 38, 982–994, 2001.

476 Finlay, P.J., Mostyn, G.R., and Fell, R.: Landslide risk assessment: prediction of travel distance,
477   Canadian Geotechnical Journal., 36, 556–562, 1999.

478 Fell, R., Corominas, J., Bonnard, C., Cascini, L., Leroi, E., and Savage, W. Z.: Guidelines for
479   landslide susceptibility, hazard and risk zoning for land use planning, Engineering Geology.,
480   102, 85–98, 2008.

481 Fannin, R., and Wise, M.: An empirical-statistical model for debris flow travel distance, Can
482   Geotech J ., 38, 982–994, 2001.

483 Glade, T.: Linking debris-flow hazard assessments with geomorphology. Geomorphology., 66(1):
484   189-213, 2005.

485 Glade, T., Anderson, M. G., Crozier, M.J.: Landslide hazard and risk. Wiley., 75-138, 2006.

486 GB 50010–2010.: Code for design concrete structures, Beijing: Chinese Architectural Industry.,
487   34–80, 2010 (in Chinese).

488 Hebei Province Institute of Hydrogeological and Engineering.: Geological investigation
489   engineering supplemental survey report of Hongse Village Taziping landslide in Hongkou
490   Town of Dujiangyan City, Sichuan Province., 2010 (in Chinese).

491 Hungr, O.: A Model for the runout analysis of rapid flow slides, debris flows and avalanches, Can
492   Geotech J ., 32, 610–623, 1995.

493 Hungr, O., Evans, S.G., Bovis, M,J., and Hutchinson, J,N.: A review of the classification of
494   landslides of the flow type, Environ Eng Geosci., 7, 221–238, 2001.

495 Hungr, O., Morgan G.C., and Kellerhals, R.: Quantitative analysis of debris torrent hazards for
496   design of remedial measures, Can Geotech J., 21, 663–677, 1984.

497 Hu, K.H., Cui, P., and Zhang, J.Q., Characteristics of damage to buildings by debris flows on 7
498   August 2010 in Zhouqu, Western China, Nat Hazards Earth Syst Sci., 12, 2209–2217, 2012.

499 Hürlimann, M., Rickenmann, D., Medina, V., and Bateman, A.: Evaluation of approaches to
500   calculate debris-flow parameters for hazard assessment, Eng Geol., 102, 152–163, 2008.

501 Huang, Y., Cheng, H., Dai, Z., Xu, Q., Liu, F., Sawada, K., Moriguchi, S., and Yashima, A.:
502   SPH-based numerical simulation of catastrophic debris flows after the 2008 Wenchuan
503   earthquake, Bull Eng Geol Environ., 74, 1137–1151, 2015.

504 Iverson, R. M., Reid, M. E., and LaHusen, R. G.: Debris-flow mobilization from landslides, Annu.
505   Rev. Earth Planet Sc., 25, 85– 138, 1997.

506 Iverson, R.M., and Vallance, J.W.: New views of granular mass flows, Geology., 29, 1115–1118,
507   2001.

508 Iovine, G., Gregorio, S,D., and Lupiano, V.: Debris-flow susceptibility assessment through cellular
509   automata modeling: an example from 15–16 December 1999 disaster at Cervinara and San
510   Martino Valle Caudina (Campania, southern Italy), Nat Hazards Earth Syst Sci., 3, 457–468,
511   2003.

512 Jackson, L.E., Kostashuk, R.A., and MacDonald, G.M.: Identification of debris flow hazard on
513   alluvial fans in the Canadian Rocky mountains, Geological Society of America., 7, 155–124,

1987.

LeVeque, R.: Finite Volume Methods for Hyperbolic Problems, Cambridge Texts in Applied Mathematics Cambridge University Press., 2002.

~~Michael,L.M., 2003. Baynes F, Scott G, Granger K Regional landsliderisk to the Cairns community[J]. NatHazards, 2003,30 (2):233–249.~~

Michael-Leiba, M., Baynes, F., Scott, G., and Granger, K.: Regional landsliderisk to the Cairns community, NatHazards., 30, 233–249, 2003.

Morgenstern, N.R., and Price, V.E.: The analysis of the stability of general slip surfaces, Geotechnique., 15, 79–93, 1965.

Portilla, M., Chevalier, G., and Hürlimann, M.: Description and analysis of the debris flows occurred during 2008 in the Eastern Pyrenees, Nat. Hazards Earth Syst. Sci., 10, 1635–1645, 2010.

Petrazzuoli, S,M., and Zuccaro, G.: Structural resistance of reinforced concrete buildings under pyroclastic flows: a study of the Vesuvian area, J Volcanol Geoth Res., 133, 353–367, 2004.

Sassa, K., Nagai, S., Solidum, R., Yamazaki, Y., and Ohta, H.: An integrated model simulating the initiation and motion of earthquake and rain induced rapid landslides and its application to the 2006 Leyte landslide, Landslides., 7, 219–236, 2010.

Scott, K.M., and Vallance, J.W.: History of Landslides and Debris Flows at Mount Rainier: Water Fact Sheet, USGS Open-File Report., 93–111, 1993.

Shi,G.H.: Discontinuous deformation analysis - a new numerical model for the statics and dynamics of block system, Berkeley: University of California., 1988.

DZ/T 0286-2015.: Specification of risk assessment for geological hazard, Ministry of Land and Resources of the People's Republic of China., 2015 (in Chinese).

Scheidl, C., and Rickenmann, D.: Empirical prediction of debris-flow mobility and deposition on fans, Earth Surf Proc Land., 35, 157–173, 2010.

Toro, E.F.: Riemann problems and the waf method for solving the two dimensional shallow water equations. Philos. Trans. R. Soc. London., Ser. A 338, 43–68, 1992.

Varnes, D.J., : Slope movement types and processes. In: Schuster RL, Krizek RJ (eds) Landslides: analysis and control. Transportation Research Board, National Research Council, Washington, DC, USA., 11–33 , 1978.

Wang, L., Li, B., Gao, Y., and Zhu, S.: Run-out prediction of large thick-bedded unstable rock: A case study of Daxiang unstable rock in Yangjiao town, Wulong county, Chongqing, Earth Science Frontiers., 23, 251–259, 2016 (in Chinese).

WSL.: RAMMS: A numerical model for snow avalanches in research and practice, User manual v1.5 avalanche, WSL Institute for snow and avalanche research SLF, Swiss., 2013.

~~Yin, K.L., Jiang, Q.H., and Wang, Y.: Simulation of Landslide Movement Process by Discontinuous Deformation Analysis, Earth Science Journal of China University of Geosciences, 27, 632–636, 2002 (in Chinese).~~

~~Zhang, Y.J.: Study on dynamic characteristics of typic rock avalanche on canyon area, Shanghai Jiao Tong University, 2013 (in Chinese).~~

~~Zhang, Z.Y., Wang, S.T., Wang, L.S., Huang, R.Q., Xu, Q., and Tao, L.J.: Principles of engineering geology, Beijing: Geology Press., 212-224, 1993 (in Chinese).~~

Zeng, C., Cui, P., Su, Z.M., Lei, Y., Chen, R.: Failure modes of reinforced concrete columns of buildings under debris flow impact, Landslides., 12, 561-571, 2015.

[a68]: Answer to the comment Q32: We have revised all references according to the NHESSD journal style. The reference list has been updated as well.

[a69]: Answer to the comment Q13: It has been cited.

[a70]: Answer to the comment Q6: We have deleted some parts of unimportant Chinese's literature and revised all references according to the NHESSD journal style.

Natural Hazards
and Earth System
Sciences

Open Access

EGU

Discussions

Interactive comment on "Hazard Assessment Comparison of Tazhiping Landslide Before and After Treatment" *by* Dong Huang et al.

Dong Huang et al.

dhuang@imde.ac.cn

Received and published: 28 June 2017

Response to Reviewer Comments

Manuscript title: (the original title: Hazard Assessment Comparison of Tazhiping Landslide Before and After Treatment) Manuscript number: 2019-391 Thanks very much for reviewer's comments, which helped us to improve the quality of manuscript. We have made major revisions to address the comments raised by the reviewer. The following responses have been prepared to address reviewer' s comments in a point-by-point fashion. All changes have been marked with RED in the revised manuscript. We would be happy to make further modifications if required. We hope the changes listed have made the manuscript suitable for publication, and we look forward to your response.

General comments

Q1: The manuscript presented a fluid mechanics based method for landslide/debris flow modeling, and was further applied to a real landslide case for hazard zones mapping. The topic is scientifically significant for nature hazard mitigations. The manuscript was logically organized and the results were well described and reasonably discussed. The authors provided sufficient evidence that the proposed method could be used as a promising tool for landslide modeling and hazard mapping. The knowledge obtained from the study would benefit civil engineering society for landslide investigation assessment. This paper can be accepted for publication by considering all the points given below.

A1: Thank you very much for the reviewer's positive comments about our work. We have addressed each comment meticulously and illuminated the requests in the following responses and the text as much as possible.

Q2: The main contribution of this paper seems to be the computational model proposed. It is desired to add related descriptions to the title of this paper.

A2: We appreciate the reviewer's suggestion. The title of this paper has been revised to "Hazard Assessment Comparison of Tazhiping Landslide Before and After Treatment Using the Finite Volume Method". Please see p.1, line 2.

Q3: Previous study on landslide/debris flow issues using the fluid mechanics based method had faced the problem that it predicts higher mobility of the moving body while using the same fluid parameters throughout the whole flowing process. For example, less obvious fluid property is expected when the flow body is approaching stop point. It is stated in this manuscript that a changed frictional resistance is used (L78). However, the details are not clear in the text. Relevant descriptions on this issue should be strengthened.

A3: This paper adopted the RAMMS to simulate the mass movement process. In

RAMMS, the friction coefficient for our calculation domain can be automatically adjusted based on topographic data analysis, forest information and global parameters. Therefore, a changed frictional resistance was applied to the slide mass during the flowing process. We added more details in the discussion section. Please see p.22-23, line 384∼411.

Q4: It is not clear in the text that how the free surface of the landslide/debris flow is treated or reconstructed. An additional figure is need to describe the details.

A4: The landslide body as well as the calculation domain were reconstructed and specified though the topographic data input with the built-in RAMMS Project Wizard. We have added new Figure 4 to show more details. Please see p.10, line 219.

Q5: Fig.4 showed the geological profile of Taziping Landslide and a slide surface is clearly indicated. Is this slide surface comparable with the simulation result? It would be interesting to show their comparison.

A5: The indicated slide surface in Fig.4 shows a potential surface before treatment. Combined with the other field survey data. It was concluded that the sliding mass had an estimated starting volume of about 600,000m3 and a mean thickness of 8m. After fully accounting for the slide-resistant piles and mounds, we introduced the Morgenstern-Price method to calculate the stability coefficient of Taziping landslide after treatment. The method was determined with an iterative approaching by changing the position of the sliding surface until failure of the dumpsite (Figure. 8). It was suggested the treatment significantly improved the slide stability. We added more descriptions on this issue. Please see p.15, line 305∼307 and 311∼312.

Q6: In Tab.3, Various hazard zone levels were cataloged. What is the criterial to assign a specific damage situation to a certain zone level? Is there any standard code to follow?

A6: The hazard zone levels were cataloged according to current standard and litera-

tures. We have cited the relevant standard code and literature (Fell R et al., 2008; DZ/T 0286-2015). Please see p.18, line 359~360.

Other specific comments are given below.

Q7: The quotations in the manuscript are not in the same format, for example, Line 44, Costa, 1984; VS Line 50, Zhang. Y, 2013. Usually only family name is preferred, please refer to the journal's instructions and make necessary changes throughout the text.

A7: Thank you for pointing out the inaccurate quotation. It has been revised. We have revised all references and quotations in the manuscript according to the NHESSD journal style. The reference list has been updated as well. Please see the references section.

Q8: Fig.1 needs proper citation.

A8: Thank you for the correction. It has been revised (Christen et al., 2010a).

Q9: In Fig.6, Fig.7, what moment of flow does these figures represent? Different moment should have different deposit thickness, flow velocity and pressure. Please confirm.

A9: Figure 6 and Figure 7 show the last moment of the flow. The flow has a different deposit flow height, velocity and pressure at various moments in time. However, the colored bar shows the maximum values of the movement process or an instantaneous for a given time step. It has been revised. Please see p.17, line 329-331.

Q10: L276 "The middle and lower deposits had a thickness of about 5-10m", confusing here, what does "the middle and lower deposits" mean? Similar as "the middle and lower movement speed", please check throughout the text.

A10: The authors apologize for the confusion. The sentences have been reformulated. Please see p.15, line 293 and 294; p.17, line 333.

Q11: L289. What technique is used for searching the sliding plane.

A11: The method coupled with field borehole surveying and the numerical calculation method described in Q5 were used to search the sliding plane.

Q12: L305, Fig.4 should be Fig.7.

A12: Thank you for the correction. It has been revised. Please see p.17, line 328.

Q13: Tab.3. How is the "Building damage probability" evaluated?

A13: Thank you for the comment. Building damage probability is evaluated by the thickness of a landslide mass that the building can withstand. We have cited the relevant literature (Hungr et al., 1984; Petrazzuoli et al., 2004; GB, 50010–2010; Hu et al., 2012; Zeng et al., 2015). Please see p18, line 362 and 364.

The text of the manuscript has been revised.

Please also note the supplement to this comment:
https://www.nat-hazards-earth-syst-sci-discuss.net/nhess-2016-391/nhess-2016-391-AC8-supplement.pdf

———————————————————

Interactive comment on Nat. Hazards Earth Syst. Sci. Discuss., https://doi.org/10.5194/nhess-2016-391, 2017.

Hazard Assessment Comparison of Tazhiping Landslide Before and After Treatment using the finite volume method

Dong Huang [1], YuanJun Jiang[1]*, JianPing Qiao[1], Meng Wang[1]

1. Key Laboratory of Mountain hazards and Surface process, Institute of Mountain hazards and Environment, Chinese Academy of Science, Chengdu 610041, China
*Corresponding author (yuanjun.jiang.civil@gmail.com).

Abstract: Through investigation and analysis of geological conditions and mechanical parameters of the Taziping landslide, the finite volume method was adopted, and, the rheological model was adopted to simulate the landslide and avalanche entire mass movement process. The present paper adopted the numerical approach of RAMMS and the GIS platform to simulate the mass movement process before and after treatment. This paper also provided the conditions and characteristic parameters of soil deposits (~~thickness~~ flow height, ~~speed~~ velocity, and stresses) during the landslide mass movement process and mapped the 3D division of hazard zones before and after landslide treatment. Results indicated that the scope of hazard zones contracted after engineering treatment of the landslide. The extent of high-hazard zones was reduced by about 2/3 of the area before treatment, and characteristic parameters of the mass movement process after treatment decreased to 1/3 of those before treatment. Despite engineering treatment, the Taziping landslide still poses significant hazard to nearby settlements. Therefore, we propose that houses located in high-hazard zones be relocated or reinforced for protection.

Keywords: finite volume method; rheological model; motion feature parameters; hazard assessment

1. Introduction

The hazards of a landslide include scope of influence (i.e., source area, possible path area, and backward and lateral expansion area) and secondary disasters (i.e., reservoir surge, blast, and landslide-induced barrier lake). A typical landslide hazard assessment aims to propose a systematic hazard assessment method with regard to a given position or a potential landslide. Current research on typical landslide hazard assessment remains immature, and there are multiple methods for interpreting landslide hazards. To be specific, the scope of influence prediction of a landslide refers to deformation and instability characteristics such as sliding distance, movement speed, and bulking thickness range. The movement behavior of a landslide mass is related to its occurrence, sliding mechanisms, mass characteristics, sliding path, and many other factors. Current landslide movement prediction methods include empirical prediction and numerical simulation.

Empirical prediction method: The empirical prediction method involves

analyzing landslide flow through the collection of landslide parameters in the field. It further consists of the geomorphologic method (Costa, 1984; Jackson et al., 1987; Scott et al., 1993), the geometric change method (Zhang et al., 1994 1993; Finlay et al., 1999; Michael-Leiba et al., 2003), and the volume change method (Fannin et al., 2001). Empirical models are commonly simple and easy to apply, and the required data are easy to obtain as well. **Numerical simulation method:** Numerical simulation methods are further divided into the continuous deformation analysis method (Hungr, 1995; Evans et al., 2009; Zhang .Y, 2013; Wang L, et al., 2016), the discontinuous deformation analysis method (Shi G.H, 1988; Yin et al., 2002), and the simplified analytical simulation method (Christen et al., 2010a; Sassa, 2010; Bartelt et al., 2012; Du et al., 2015). The numerical simulation method expresses continuous physical variables using the original spatial and temporal coordinates with geometric values of discrete points. Numerical simulations follow certain rules to establish an algebraic equation set in order to obtain approximate solutions for physical variables.

Empirical prediction models only provide a simple prediction of the sliding path. Due to the differences in geological environments, empirical prediction models commonly have low generality. The continuous deformation method has the advantage of an extremely strong replication capability, but it is not recommended when analyzing flow-type landslides debris flows, lahars, or debris flows because of complicated rheological behaviors (Iverson et al., 1997, 2001; Hungr et al., 2001; Glade 2005; Portilla et al., 2010;Chen et al., 2014). The fluid mechanics-based discontinuous deformation method has several shortcomings such as, great computational burden, difficult parameter selection, and difficult 3D implementation. The simplified analytical simulation method fully takes into account the flow state properties of landslides before introducing a rheological model and can easily realize 3D implementation on the GIS platform. On that account, this paper adopted the continuous fluid mechanics-based finite volume method (simplified analytical simulation method). We introduce a rheological model on the basis of using mass as well as momentum and energy conservation to describe the movement of landslides. We also employed GIS analysis to simulate the entire movement process of Taziping landslide and map the 2D division of hazard zones.

2. Methods

2.1 Kinetic analysis method

Adopting the continuous fluid mechanics-based finite volume method, this paper took into account erosion action on the lower surface of the sliding mass and the change in frictional resistance within the landslide-debris flow in order to establish a computational model. The basic idea is to divide the calculation area into a series of non-repetitive control volumes, ensuring that there is a control volume around each grid point. Each control volume is then integrated by the unresolved differential equation in order to obtain a set of discrete equations. The unknown variable is the numerical value of the dependent variable at each grid point. To solve the integral of a control volume, we make a hypothesis about the change rule of values among grid
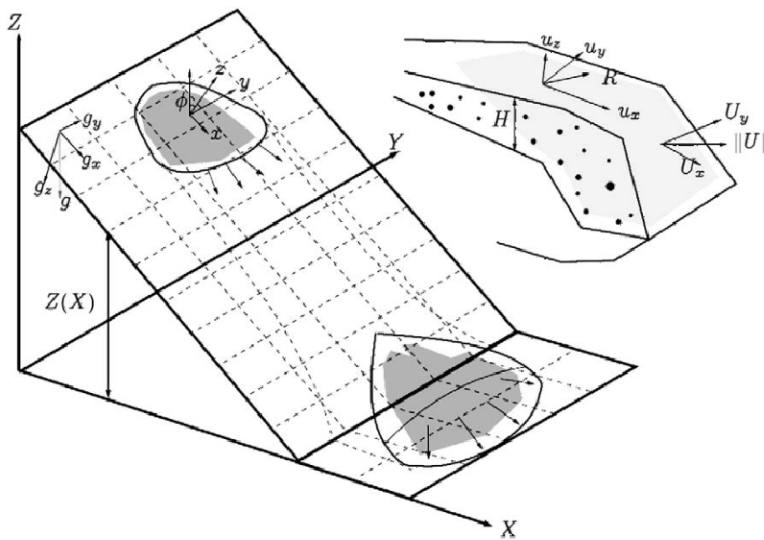
[a2]: Answer to the comment Q7: It has been revised. We have revised all references and quotations in the manuscript according to the NHESSD journal style.

[a3]: Answer to the comment Q7: It has been revised.

[a4]: Answer to the comment Q7: It has been revised.

87 points, that is, about their piecewise distribution profile. The finite volume method
88 can satisfactorily overcome the finite element method's weakness of slow calculation,
89 and solve the problem of complex region processing. Thus, we adopted the finite
90 volume method to establish the kinematic model for the landslide flow process.

91   The core of the finite volume method is domain discretization. The finite volume
92 method uses discrete points as a substitute for continuous space. The physical
93 meaning of the discrete equation is the conservation of the dependent variable in a
94 finite control volume. Establishment of the conservation equation is based on the
95 continuous movement model, that is, the continuity hypothesis about landslide
96 substances. We divided the landslide mass into a series of units and made the
97 hypothesis that each unit has consistent kinematic parameters (speed at a depth,
98 density, etc.) and physical parameters (Fig.1). We also established an Eulerian
99 coordinate system-based conservation equation with regard to each control volume.

100

101   Fig.1 Schematic diagram of finite volume discretization (Christen et al., 2010a).

102 **2.2 Control equation**

103   The computational domain is defined as directions x and y, and the

104 topographic elevation is given the coordinate $z(x,y)$. $H(x,y,t)$ is assumed as the

105 change relationship of landslide thickness with time; $U_x(x,y,t)$ and $U_y(x,y,t)$

106 respectively represent the mean movement speeds along directions x and y at

107 moment t; $n_x = U_x / \sqrt{U_x^2 + U_y^2}$ and $n_y = U_y / \sqrt{U_x^2 + U_y^2}$ represent the cosinoidal and

108 sinusoidal flow vectors of the landslide on the plane x-y. The mean flow speed of

[a5]: Answer to the comment Q8: It has been revised (Christen et al., 2010a).

3

109   substances is defined as $U = \sqrt{U_x^2 + U_y^2}$.

110   Thus, the mass balance equation becomes:

111
$$\partial_t H + \partial_x (HU_x) + \partial_y (HU_y) = \dot{Q} \tag{1}$$

112   wherein, $\dot{Q}(x,y,t)$ represents the change rate (entrainment rate) of landslide

113   volume with time.

114   Assuming that $l(x,y,t)$ represents the movement distance of the landslide with

115   time, we can obtain:

116
$$\dot{Q} = \begin{cases} 0 & if & h_i = 0 \\ \dfrac{\rho_i}{\rho_a} h_i \dfrac{U}{l} & if & k_i l \geq h_i \\ \dfrac{\rho_i}{\rho_a} k_i U & if & k_i l < h_i \end{cases} \tag{2}$$

117   wherein, h_i represents the thickness of the i th layer of the landslide in the

118   movement process; ρ_i represents the density of the i th layer of the landslide in the

119   movement process; ρ_a represents the density of the landslide; the dimensionless

120   parameter k_i represents the entrainment rate.

121   The momentum balance equation is:

122
$$\partial_t (HU_x) + \partial_x (HU_x^2 + \frac{g_z k_{a/p} H^2}{2}) + \partial_y (HU_x U_y) = S_{gy} - S_f(R)[n_x] \tag{3}$$

123
$$\partial_t (HU_y) + \partial_y (HU_y^2 + \frac{g_z k_{a/p} H^2}{2}) + \partial_x (HU_x U_y) = S_{gx} - S_f(R)[n_y] \tag{4}$$

124   wherein, $S_{gx} = g_x H$ and $S_{gy} = g_y H$ represent the dynamic components of the

125   acceleration of gravity in directions x and y ; $g = (g_x \quad g_y \quad g_z)$ represents the

126   vector of the acceleration of gravity; $k_{a/p}$ represents the pressure coefficient of soil;

127   ρ_a represents the density of the landslide; the dimensionless parameter k_i

128   represents the entrainment rate; $S_f(R)$ represents the frictional resistance.

129   The kinetic energy balance equation is:

130
$$\partial_t (HR) + \partial_x (HRU_x) + \partial_y (HRU_y) = \dot{P} - \dot{D} \tag{5}$$

131   wherein, $R(x,y,t)$ represents the random mean kinetic energy of the landslide;

132     $\dot{P}(x,y,t)$ and $\dot{D}(x,y,t)$ represent the random increased kinetic energy and decreased

133 kinetic energy of the landslide.

2.3 Constitutive relationship

135   The improved Voellmy rheological model is applied in the computational

136 simulation of the landslide. See the computational formula below:

$$S_f = \frac{u_i}{\|U\|}\left(h\mu g_z + R_t U^2 + R_\zeta U^2\right) \tag{6}$$

$$R_t = \mu h \frac{U^T K U}{U^2}, R_\zeta = \frac{g}{\zeta} \tag{7}$$

139   wherein, $u_i/\|U\|$ represents the unit vector in the movement direction of the

140 landslide; μ represents the Coulomb friction coefficient, and is related to $R(x,y,t)$,

141 the random mean kinetic energy of the landslide; R_t represents the gravity-related

142 frictional force coefficient; K represents the substrate surface curvature; ζ

143 represents the viscous friction coefficient of the "turbulent flow".

2.4 HLLE-Heun numerical solution

145   Synthesizing control equations (1), (3), (4) and (5), we can obtain the simplified

146 form of the nonlinear hyperbola equation:

$$\partial_t V + \nabla \cdot F(V) = G(V) \tag{8}$$

$$V = \begin{pmatrix} H \\ HU_x \\ HU_y \\ HR \end{pmatrix} \qquad G(V) := \begin{pmatrix} \dot{Q} \\ S_{gx} - S_{fx} \\ S_{gy} - S_{fy} \\ \dot{P} - \dot{D} \end{pmatrix}$$

$$F(V) = \begin{pmatrix} HU_x & HU_y \\ HU_x^2 + g_z k_{a/p} \dfrac{H^2}{2} & HU_x U_y \\ HU_x U_y & HU_y^2 + g_z k_{a/p} \dfrac{H^2}{2} \\ HRU_x & HRU_y \end{pmatrix}$$

150   wherein, $V(x,y,t)$ represents a vector equation consisting of four unknown

151 vector variables; $F(V)$ represents the flux function; $G(V)$ represents the source

152 term. Based on the HLLE equation of the finite volume method and the quadrilateral

153 grid, the node layout can adopt the grid center pattern, and the normal flux along one

154 side of the control volume can be represented by the flux at the center of the side. The

155 finite volume discretization adopting the control volume as unit is depicted in Fig.1;

156 the Gauss theorem can be followed for the integration of equation (8), wherein C_i

157 represents the unit volume; after converting the volume integral flux function $F(V)$

158 into the curved surface integral, we can obtain:

159
$$\int_{C_i} \partial_t V dx + \iint_{\partial C_i} F(V) \cdot n_i d\sigma = \int_{C_i} G(V) dx \tag{9}$$

160 wherein, n_i represents the outward normal direction vertical to unit C_i at the

161 boundary; through adopting the HLL format for the discretization of surface integral,
162 the following simplified form can be obtained:

163
$$V_i^{(*)} = V_i^{(n)} + \frac{\Delta t}{A_{C_i}} \Delta F_i^{(HLL)}\left(V^{(n)}\right) \tag{10}$$

164
$$V_i^{(**)} = V_i^{(*)} + \frac{\Delta t}{A_{C_i}} \Delta F_i^{(HLL)}\left(V^{(*)}\right) \tag{11}$$

165
$$V_i^{(n+1)} = \frac{1}{2}\left(V_i^{(n)} + V_i^{(**)}\right) \tag{12}$$

166 wherein, $V_i^{(n)}$ represents the mean value of unit variables at moment $t^{(n)}$; $V^{(n)}$

167 represents the mean value of the entire grid at moment $t^{(n)}$; $\Delta t := t^{(n-1)} - t^{(n)}$ represents

168 the calculated time step; A_{C_i} represents the area of unit C_i; $\Delta F_i^{(HLL)}$ represents the

169 approximate value of the curved surface integral, as shown below:

170
$$\Delta F_i^{(HLL)}\left(V^{(n)}\right) := -\sum_{j=1}^{4} F_{ij}^{(HLL)}\left(V^{(n)}\right) n_{ij} \Delta X \tag{13}$$

171 wherein, n_{ij} represents the outward normal direction of the i th unit at

172 boundary j; the flux calculation term $F_{ij}^{(HLL)}\left(V^{(n)}\right)$ represents the approximate

173 solution mode of the Riemann problem of the i th unit at boundary j; see the

174 computational formula below:

175
$$F_{ij}^{(HLL)}\left(V^{(n)}\right) = \begin{cases} F\left(V_L^{(n)}\right) & 0 \le S_L \\ \dfrac{S_R F\left(V_L^{(n)}\right) - S_L F\left(V_R^{(n)}\right) + S_R S_L F\left(V_R^{(n)} - V_L^{(n)}\right)}{S_R - S_L} & S_L \le 0 \le S_R \\ F\left(V_R^{(n)}\right) & S_R \le 0 \end{cases} \tag{14}$$

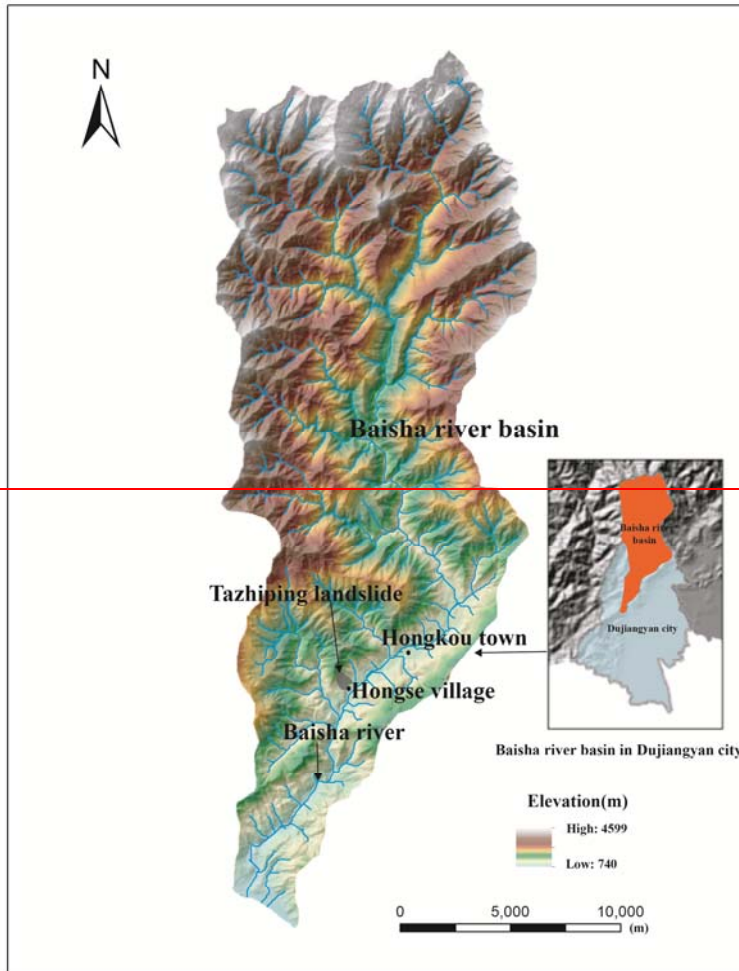176 wherein, $V_L^{(n)}$ and $V_R^{(n)}$ respectively represent the approximate values of $V^{(n)}$

177 on both sides of boundary j of the i th unit; S_L and S_R respectively represent the

178 wave speeds on the left and right sides. Refer to the computational method described

179 by Toro (1992). In addition, the gradient magnitude in the original second-order

180 difference equation can be limited through multiplication with the flux limiter, and the

181 second-order format of the TVD property can be constructed to avoid the occurrence

182 of numerical oscillation. Refer to the specific method described by LeVeque (2002).

183 In this paper a numerical solver ~~used~~ within RAMMS is used, which was

184 specifically designed to provide landslide (avalanche) engineers with a tool that can

185 ~~be applied to~~ analyze problems ~~that~~ with two-dimensional depth-averaged mass and

186 momentum equations on three-dimensional terrain using both first and second-order

187 finite volume methods (Christen et al., 2010b).

3. Study area and data

3.1 Taziping landslide

190 The Taziping landslide is located ~~in the~~ southeast of the Hongse Village,

191 Hongkou Town, Dujiangyan City of Sichuan Province. The site is located at

192 (E103°37′46″, N31°6′29″), 68 km ~~away from~~west Chengdu City ~~to the east~~ and 20

193 km ~~away~~ from the Dujiangyan Urban District (Fig. 2). Its geomorphic unit is a

194 middle-mountain tectonic erosional area~~, falling within the slope geomorphology~~ on

195 the north bank of the Baisha River Valley. ~~As an colluvial layer landslide triggered by~~

196 ~~the Wenchuan Earthquake,~~The Taziping Landslide is a large-scale colluvial layer

197 landslide triggered by the Wenchuan Earthquake~~landslide as shown in~~ (Fig. 3). It has

198 a gradient of 25°-40° with an average gradient ~~of about~~ 32°. The landslide has an

199 apparent round-backed armchair contour ~~, and has formed~~with a steep rear edge,

200 which has a gradient of 35°-50° and an elevation of about 1,370 m. The front edge is

201 located on the south side of the mountain road, and has an elevation of about 1,007 m.

202 The landslide has an elevation difference of about 363 m, and ~~the~~ a main sliding

203 direction of 124°NE. The landslide mass ~~is in~~forms an irregular semi-elliptical shape,

204 and has a length of about 530 m, an average width of 145 m and a~~n~~ ~~landslide~~ area of

205 approximately 7.68×10^4 m^2. The landslide mass is composed of gravelly soil~~ in~~

206 ~~lithology,~~ and is covered on ~~the surface~~ by silty clay mingled with gravel~~s~~. In terms of

207 spatial distribution, ~~it~~ the landslide is thick in the middle and thin on the lateral edges,

208 ~~and~~ has a thickness of 20-25 m and a volume of approximately 1.16×10^6 m^3. During

209 the earthquake, the landslide mass slid to cover the northern mountain slope ~~mass~~ of

210 the Hongse Village Miaoba settlement. The landslide has an apparent front edge

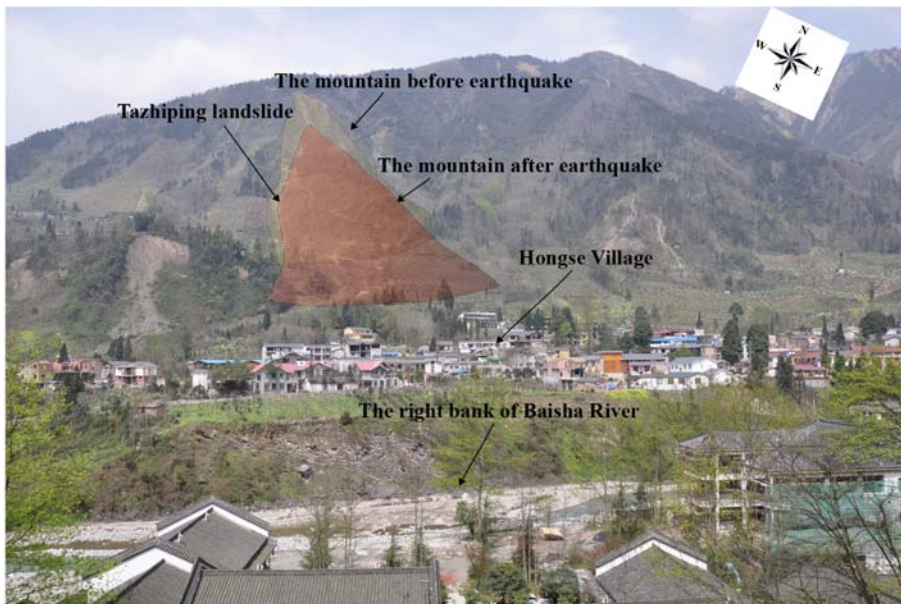211 boundary, and there is also a swelling deformation (Fig. 4).

Baisha river basin

Tazhiping landslide

Hongkou town

Hongse village

Baisha river

Baisha river basin in Dujiangyan city

Elevation(m)

High: 4599

Low: 740
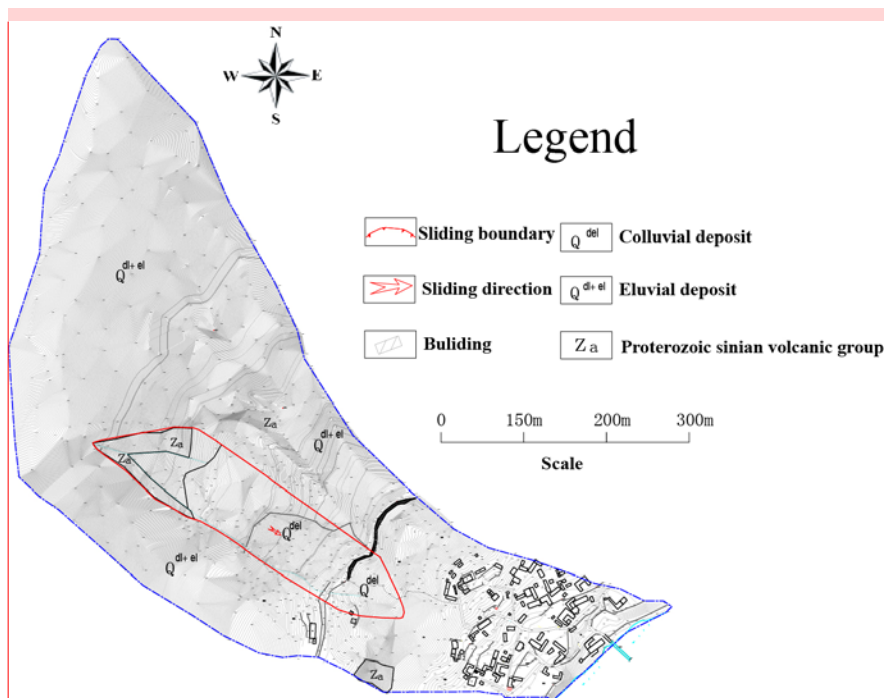
0　5,000　10,000 (m)

212

213

214   Fig.2 Location of Tazhiping landslide, Baisha river basin, Dujiangyan city (the
215   landslide was triggered by Wenchuan Ms 8.0 earthquake on May 12, 2008)

216

Fig.3 Taziping Landslide
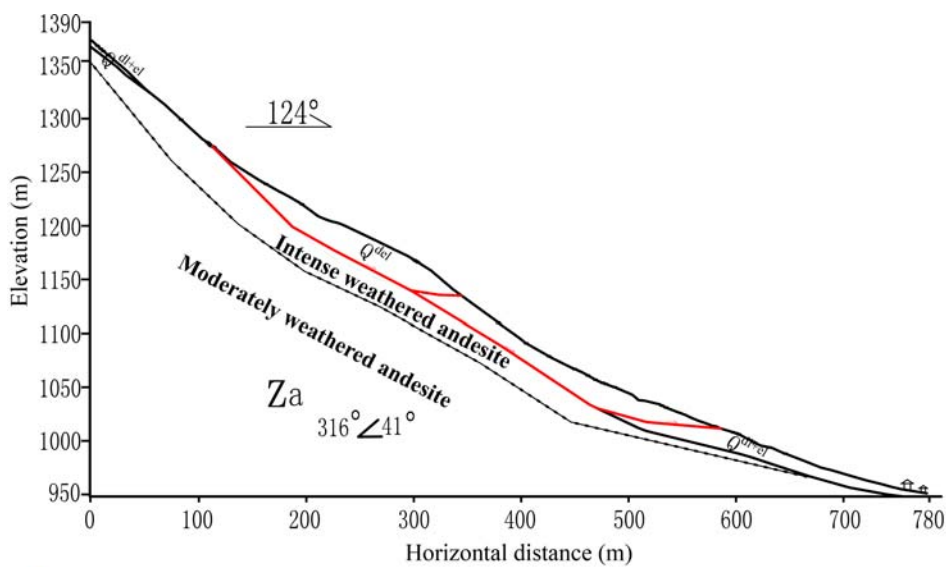
218

219 Fig.4 Plane sketch of the Tazhiping landslide

220 After the Wenchuan Earthquake, the massive colluvial deposits covers covered
221 on the mountain slope, and the landslide mass is dominated by the colluvium. The
222 colluvium is mainly distributed on the top surface of the landslide mass in the

223 ~~thickness of~~ 0.5-5.0 m thick at the top of the slide~~,~~ and is ~~mainly constituted~~
224 ~~by~~composed of rubble~~s~~ and gravel~~s~~. The mass consists of a small amount of fine
225 gravel, ~~substances~~ which ~~are~~ is composed of gray or grayish-green~~,~~ ~~and dominated by~~
226 andesite ~~in composition, generally~~ with a ~~block size~~clast of 20-150 cm. Field survey~~s~~
227 indicate~~s~~ that the rubble~~s~~ in the surface layer ~~have~~ has a maximum diameter
228 exceeding 2 m, and that fine gravel ~~substances are filled among rubbles in a loose~~
229 ~~structure~~is loosely intercalated with the rubble. ~~Within the thickness of 5-10 m, the~~
230 ~~landslide mass is constituted of a~~A small amount of yellowish-brown and gray-brown
231 silty clay ~~mingled~~ mixed with 5-40% of non-uniformly distributed ~~broken~~ rubble
232 composed the first 5-10 m of the slide.~~s~~ ~~Within the thickness of~~From 10-25 m deep,
233 there is a wide distribution of gravelly soil. The soil is grayish-green or variegated in
234 color, is slightly compact and non-uniform, and has a ~~broken stone~~rock fragment
235 content of about 50%. The parent rock of the ~~broken stones~~rock fragments is andesite,
236 filled with silty clay or silt (Fig.~~4~~ 5). Table 1 shows the parameters of the surface
237 gravelly soil of the landslide mass based on the field sampling.

238 Tab.1 Parameters of ~~the~~ surface soil of Taziping Landslide

Internal friction angle (°)		Cohesion (kPa)	Relative compactness	Natural void ratio	Dry density (kN·m⁻³)	Specific gravity (g·cm⁻³)
Peak	Residual					
27.5	23	20.5	53%	0.789	15.357	2.492

239 slide surface | Q^del colluvial deposit | Q^dl+el eluvial deposit | Z_a proterozoic sinian volcanic group
240 Fig.~~4~~ 5 Geological profile of the Taziping Landslide

241 The landslide is an unconsolidated mass containing relatively large amounts of
242 crushed stones and silty clay (Fig.~~5~~ 6). Its loose structure and strong permeability
243 facilitate infiltration of surface water. The Wenchuan earthquake aggravated the

deformation of the landslide making deposits more unconsolidated, further reducing the stability of the landslide mass. During persistent rainfall, surface water infiltrates the landslide slope resulting in increased water pressure within the landslide mass and reduced shear strength on the sliding surface. Thus, rainfall constitutes the primary inducing factor of the upper Taziping landslide. After infiltrating the loose layer, water saturates the slope increasing the dead weight of the sliding mass and reducing the shear strength of soil in the sliding zone. Infiltration into the landslide mass also increases the infiltration pressure of perched water, drives deformation, and poses a great threat to villages located at the front of the landslide. Slide-resistant piles and backfill were place at the toe of the slope in order to reduce the hazards of future slides. The slide-resistant piles have enhanced the overall stability of the slope, however, under heavy rainfall the upper unconsolidated landslide deposits may cut out from the top of the slide-resistant piles.

(a) Material on the landslide surface   (b) Material in the shear zone

Fig.5 6 Photographs showing Colluvial colluvial deposits covers on the mountain slope

Therefore we simulate possible movement states of the Taziping landslide before and after treatment with slide-resistant piles, comparatively analyzed the kinetic parameters in the movement process, and mapped the 32D division of hazard zones.
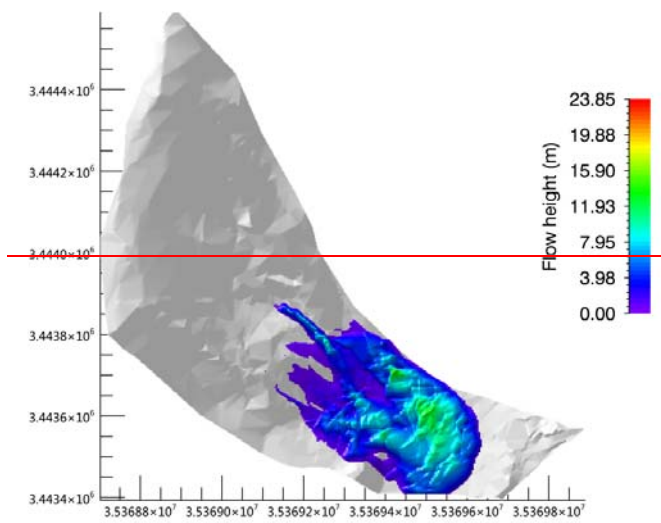
3.2 Hazard prediction before treatment

It was assumed that the landslide was damaged before engineering treatment. According to field investigation, the sliding mass had an estimated starting volume of about 600,000m^3 and a mean thickness of 8m. Based on the survey report and field investigation (Hydrologic Engineering and Geological Survey Institute of Hebei Province, 2010), we adopted the survey parameters of Tab.2 for the simulated calculation. These parameters were obtained from laboratory or small-scale experiments and back-analyses of relatively well-documented landslide cases. The unit weigh $\gamma = 20.8kN \cdot m^{-3}$ is from small-scale conventional triaxial test experiments in laboratory. In addition, we selected the coulomb friction coefficient $\mu = 0.45$ and viscous friction coefficient $\zeta = 500m \cdot s^{-2}$ in accordance
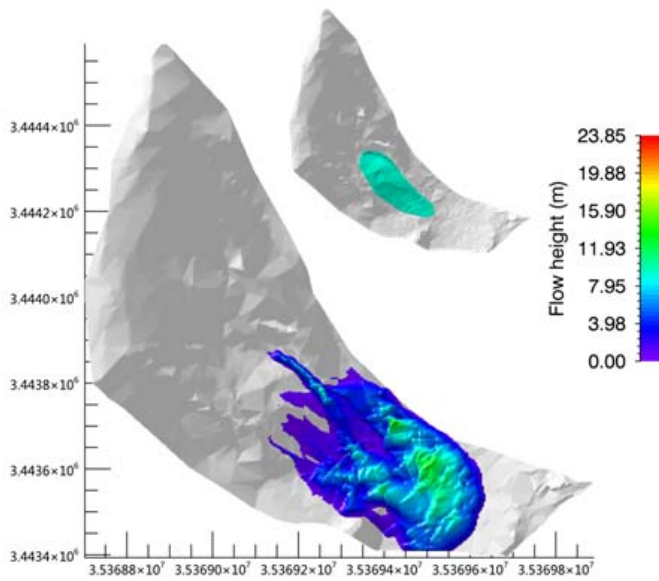
with back-analyses of well-documented landslide cases (Cepeda et al., 2010; Du et al.,
277 2015). The erosional entrainment rate selected was the minimum value $k_i = 0.0001$
278 in the RAMMS program.

279 <div align="center">Tab.2 Model calculation parameters</div>

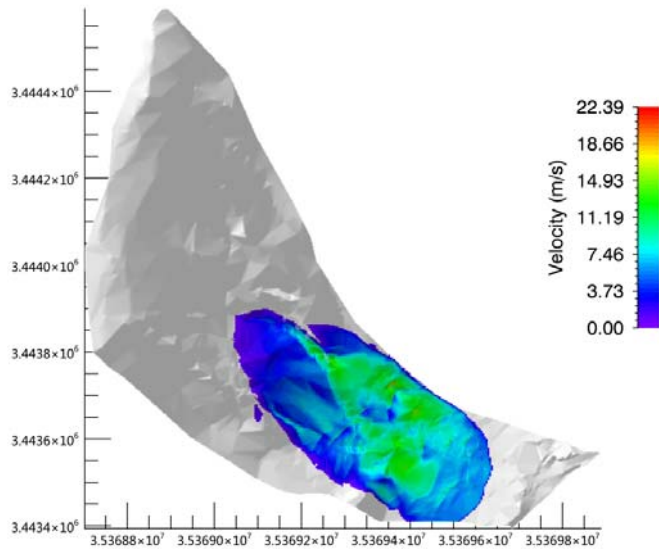| Unit weight $\gamma(kN \cdot m^{-3})$	Coulomb friction coefficient μ	Viscous friction coefficient $\zeta(m \cdot s^{-2})$	Erosional entrainment rate k_i
20.8	0.45	500	0.0001

280

281
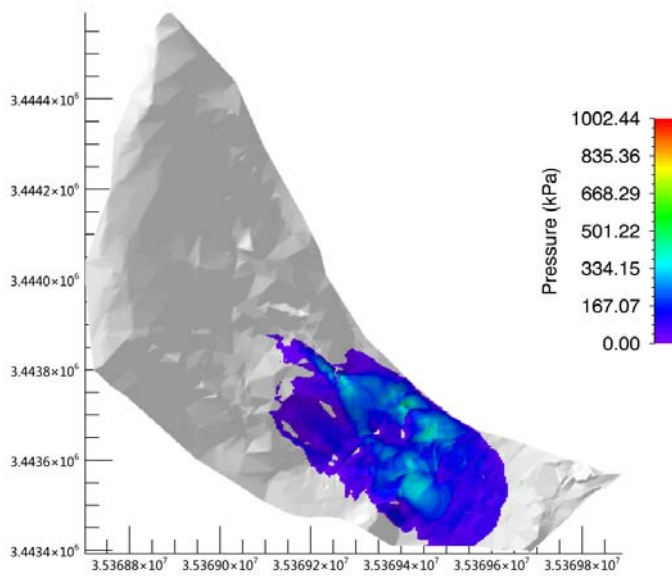
13

282

(a) ~~Thickness~~ Flow height

283

284

(b) ~~Speed~~ Velocity

285

286

(c) Pressure

287   Fig.~~6~~7   Movement characteristic parameters of the Taziping landslide (before

288   treatment)

289   See the kinematic characteristic parameters of the landslide deposits in Fig.~~6~~ 7.

290   The colored bar shows the maximum values of the kinematic process for a given time

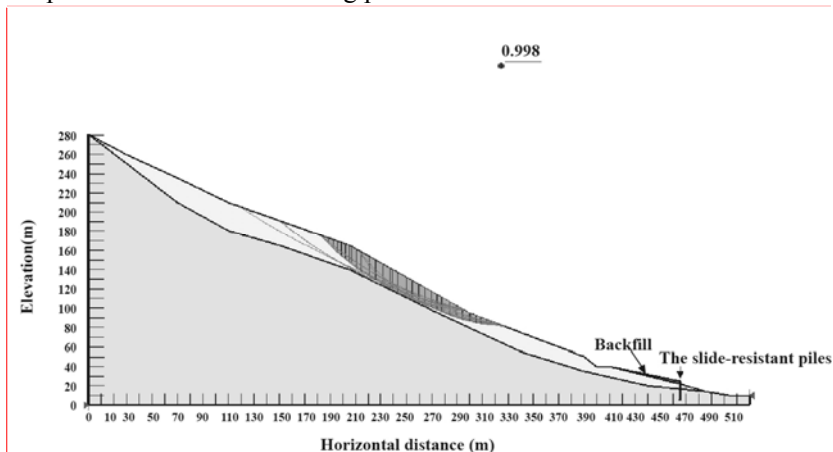291   step. As shown by the calculation results, ~~①~~ deposits accumulated during the

14

[a7]: Answer to the comment Q9: Figure.7 is shown that the last moment of the flow. Different moment have different deposit flow height, velocity and pressure. However, the coloredbar shows the maximum values of mowing process or an instantaneous for a given time step. It has been revised.

landslide movement process had a maximum ~~thickness~~ flow height of 23.85m, located around the surface gully of the middle and upper slope. The middle and lower section of the landslide deposit~~s~~ had a ~~thickness~~ flow height of about 5-10m; ② the middle and lower movement ~~speed~~ velocity of the landslide ranged from 3m/s and 7m/s; ③ the landslide had a mean pressure of about 500kPa, and the pressure of the middle and lower deposits was about 200kPa. Thus, three-story and lower houses within the deposition range might be buried, and it was further suggested that the design strength of the gable walls of houses on the middle and upper parts of the deposit be increased above 300kPa.

3.3 Hazard prediction after treatment

After fully accounting for the slide-resistant piles and mounds, we introduced the Morgenstern-Price method (Morgenstern et al., 1965) to calculate the stability coefficient of Taziping landslide after treatment. The method was determined with an iterative approach by changing the position of the sliding surface until failure of the dumpsite (Fig.8). The physico-mechanical parameters under a saturated state (Hydrologic Engineering and Geological Survey Institute of Hebei Province, 2010) were adopted to search for the sliding plane of the landslide.

Fig.8 Search for the sliding plane of the Taziping landslide (after treatment)

Based on numerical analysis, the Taziping landslide stability coefficient is 0.998. Under rainfall conditions, the middle area of the Taziping landslide was unstable. Loose deposits in the middle part of the landslide might convert into a high-water landslide ~~substances~~ and cut out from the top of the slide-resistant piles. In the damaged area, the slope had a rear edge wall elevation of about 1,170m. Its front edge was located on the south side of the mountain road, with an elevation of ~~about 1,070m~~ 1,070-1,072m and a length of ~~about 180m~~182m. Thus, the scale of the rainfall-damaged is estimated to be about 250,000m^3, with a mean thickness of about 6m. The parameters in Tab.2 were again adopted for the simulated calculation.

[a8]: Answer to the comment Q10: This sentences has been reformulated, because of wrong word order.

[a9]: Answer to the comment Q5 and Q11: Before engineering treatment, Figure.4 and Figure.5 have showed that the sliding mass had an estimated starting volume of about 600,000m^3 and a mean thickness of 8m. After fully accounting for the slide-resistant piles and mounds, we introduced the Morgenstern-Price method to calculate the stability coefficient of Taziping landslide after treatment. The method was determined with an iterative approaching by changing the position of the sliding surface until failure of the dumpsite (Figure.8)
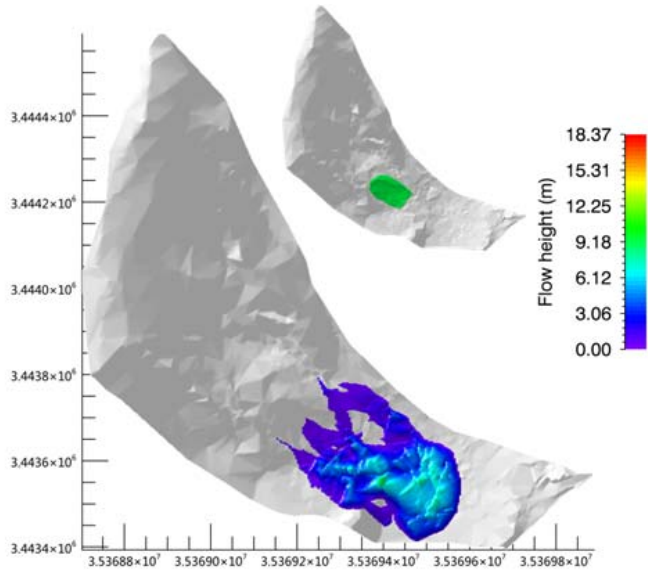
[a10]: Answer to the comment Q5: We have reconstructed and added Figure8.

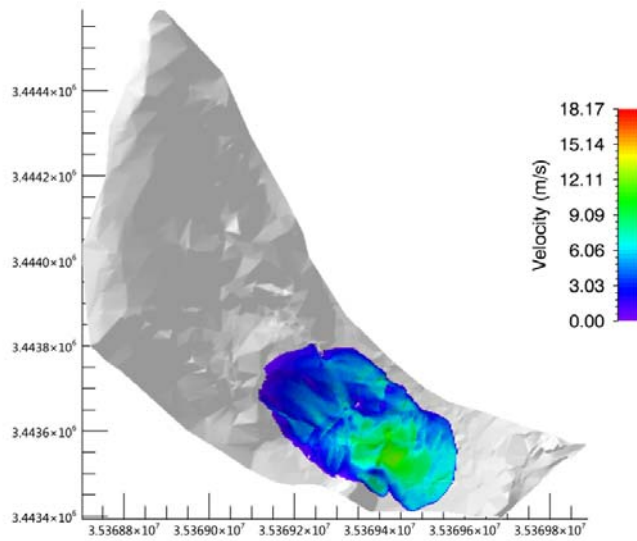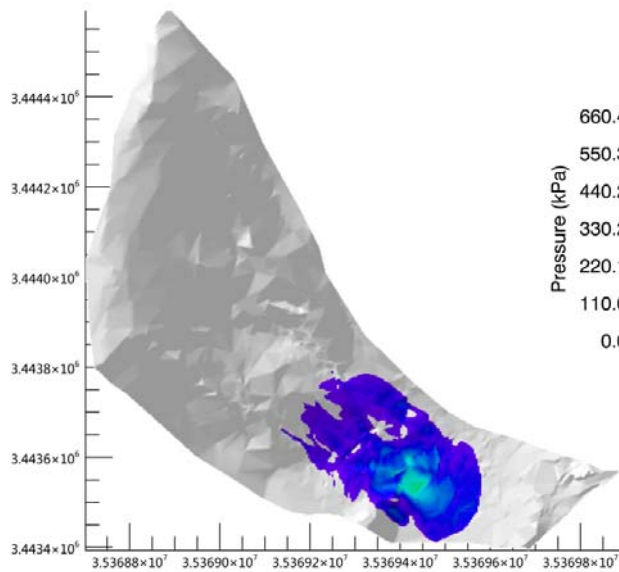[a11]: Answer to the comment Q5:The result of numerical analysis.
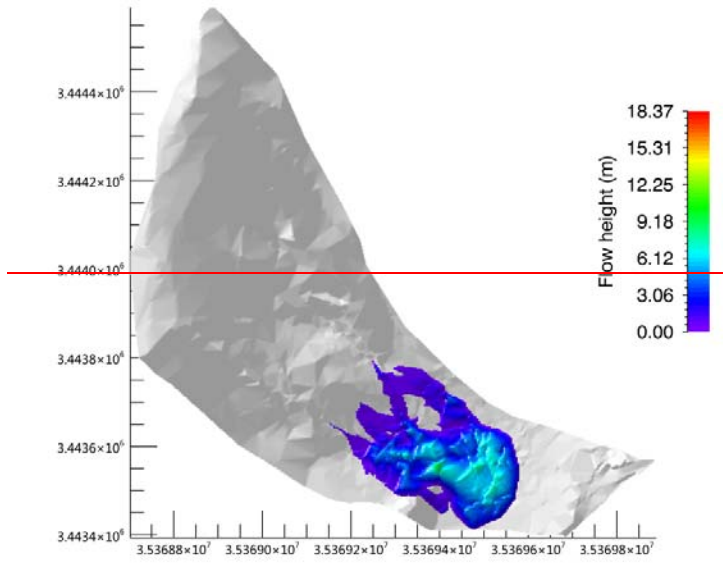
15

321

322

323   (a) ~~Thickness~~ Flow height

324

325 (b) ~~Speed~~ Velocity

326

327 (c) Pressure

328 Fig.~~7~~ 9 Movement characteristic parameters of the Taziping landslide (after treatment)

329   Provided in Fig.~~4~~ 9 are the kinematic characteristics of the landslide deposit. The

330 coloredbar shows the maximum values of moving process or an instantaneous for a

331 given time step.① Deposits accumulated during the landslide movement process had

332 a maximum ~~thickness~~ flow height of 18.37m, located around the surface gully of the

333 middle and upper slope. The middle and lower portions of the landslide deposit~~s~~ had

334 a ~~thickness~~ flow height of approximately 3-5m. ② The middle and lower movement

17

335 ~~speed~~ velocity of the landslide deposits ranged between 3m/s and 5m/s. ③ The
336 landslide had a mean pressure of about 330kPa, and the pressure of the middle and
337 lower deposits was about 100kPa. Thus, it could be held that two-story and lower
338 houses within the deposition range might be buried. It ~~was~~ is further suggested that
339 the design strength of the gable walls of houses on the middle and upper parts of the
340 deposits be increased above 150kPa.

341 After treatment, the accumulation ~~thickness~~ flow height and pressure of the
342 deposits were reduced by about 1/2, and the kinematic speed was reduced by about
343 1/3. However, the Miaoba residential area of Red Village was still partially at hazard.
344

345 **4 Results**

346 Landslides reflect landscape instability that evolves over meteorological and
347 geological timescales, and they also pose threats to people, property, and the
348 environment. The severity of these threats depends largely on landslide speed and
349 travel distance. There may be examples where entire houses on a landslide mass are
350 moved but not destroyed because of stable base plates. In any case, velocity plays a
351 more important role regarding kinetic energy acting on an obstacle. However, the
352 Miaoba residential area of Red Village is located at the frontal part of Tazhiping
353 lanslide. During landslide movement, the spatial scale indexes of a landslide mass
354 include area, volume, and thickness. The maximum thickness of the landslide is one
355 of the direct factors influencing the building's deformation failure status. A large
356 landslide displacement may lead to burial, collapse, or deformation failure of the
357 building, and thus influence its safety and stability. Thus, landslide thickness
358 constitutes an important index for assessing the hazards of a landslide disaster, and for
359 influencing the consequences faced by disaster-affected bodies (Fell et al., 2008;
360 DZ/T, 0286-2015). Provided in Tab.3 is a landslide thickness-based division of the
361 predicted hazard zones of Taziping landslide, in which the thickness of the landslide
362 mass correlates with the ability of a building to withstand a landslide disaster (Hungr
363 et al., 1984; Petrazzuoli et al., 2004; Glade 2006; GB, 50010–2010; Hu et al., 2012;
364 Zeng et al., 2015). After treatment with slide-resistant piles, the hazard of a future
365 slide was reduced by about 1/3 overall and by 2/3 in high-hazard zones.

366 **Tab.3 Division table of the predicted hazards of Taziping landslide (unit: m^2)**

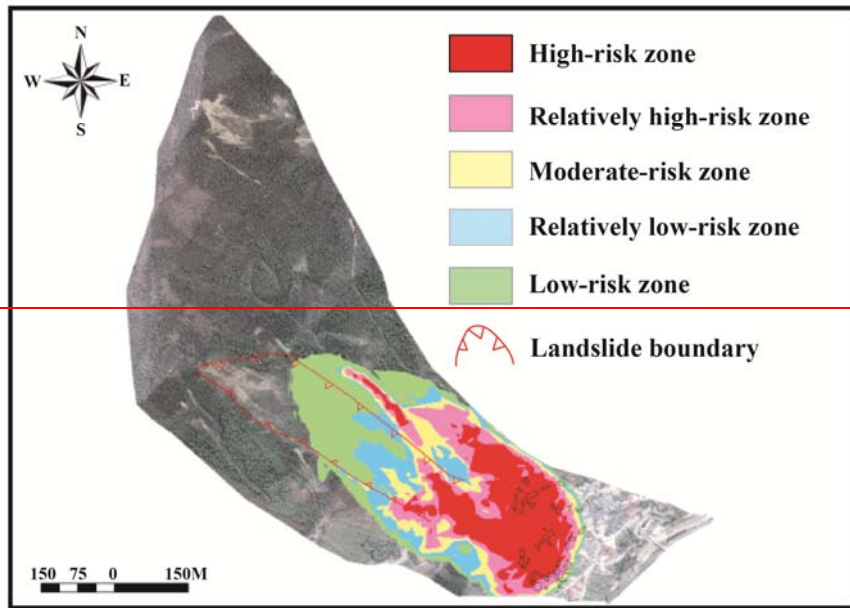| Hazard zone level	Assessment index	Building damage probability	Area before treatment	Area after treatment	Increased/decreased area	Building damage characteristics
Low-hazard zone (l)	$h \leq 0.5$m	20%	44，600	38，748	-5,852	One-story houses may be damaged; houses on the

[a15]: Answer to the comment Q6: We have cited standard code and literature.

[a16]: Answer to the comment Q13:By the thickness of the landslide mass to evaluate the ability of a building to withstand a landslide disaster. We have cited relevant literatures.
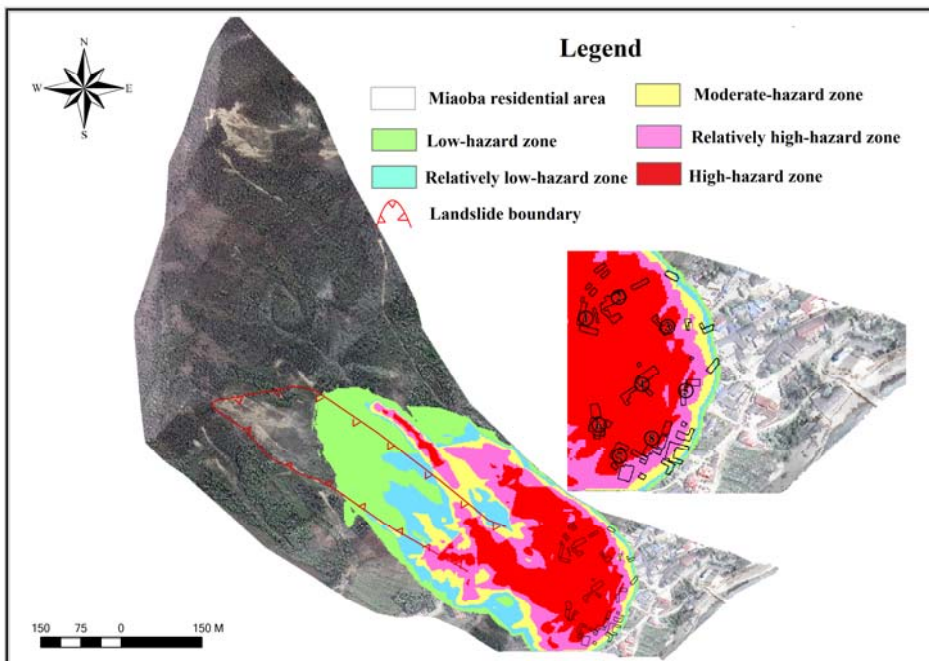
18

						landslide mass are partially damaged. One-story houses have a very high probability of being ~~washed away~~ damaged; one-story houses on the landslide mass are completely damaged.
Relatively low-hazard zone (II)	0.5 m < h≤1m	50~20%	24，900	26，400	+1,500	
Moderate-hazard zone (III)	1m < h≤3m	80~50%	21，980	15，856	-6,124	One-story to three-story houses have a very high probability of being ~~washed away~~ damaged; houses less than three stories on the landslide mass are completely damaged.
Relatively high-hazard zone (IV)	3m < h≤5m	100~80%	30，820	19，636	-11,184	One-story houses may be buried, and two-story to six-story houses have a very high probability of being ~~washed away~~

High-hazard zone (V)	$h{\geq}5$m	100%	47，240	13，052	-34,188	damaged; houses on the landslide mass are completely damaged. Two-story and lower houses may be buried, and three-story and higher houses have a very high probability of being ~~washed away~~ damaged; houses on the landslide mass are completely damaged.
Total area:	—	—	169，540	113，700	-54,340	—

Given in Fig.~~8~~ 10 are the ~~3~~2D divisions of hazard zones of <u>the</u> Taziping landslide before and after engineering treatment. The ~~scope~~ size of the hazard zones changed ~~before and~~ after engineering treatment, particularly in the high-hazard zones. Before treatment with slide-resistant piles, the landslide posed a great hazard to eight houses on the left side of the upper Miaoba residential area, with a high-hazard zone associated with landslide mass height over 5m and a red zone. After treatment, the number of effected houses was reduced to four. We defined outside the colored area as no-hazard.

375

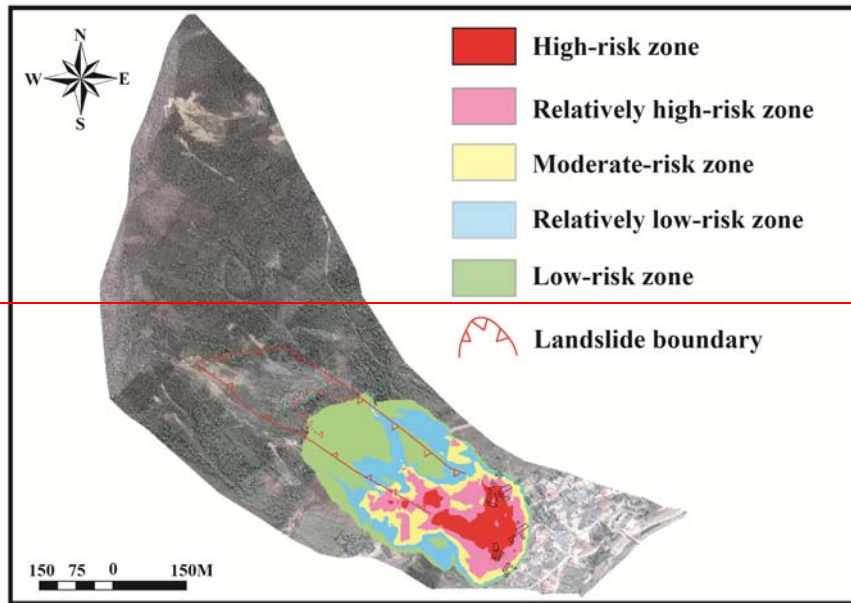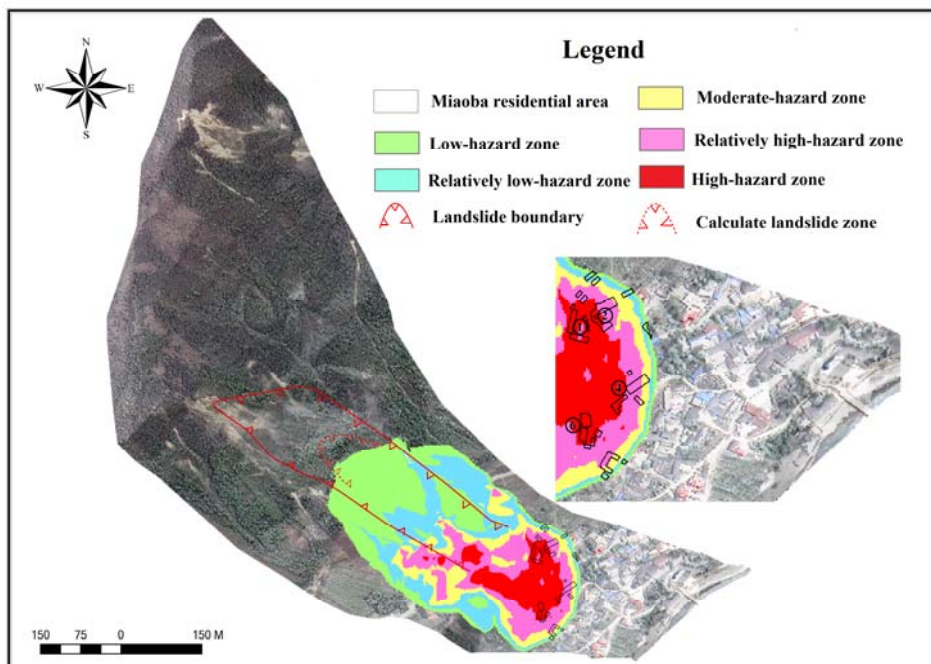376

377 **(a) Before treatment**

378

379

(eb) After treatment

Fig.810 32D division comparison of the hazards of the Taziping landslide

5 Conclusions and Discussion

The hazard assessment of landslides using numerical models is becoming more and more popular as new models are developed and become available for both

22

scientific research and practical applications. There is some confusion about the mass movement process that is discussed by the rheological model presented in this contribution.

Landslides move downslope in many different ways (Varnes, 1978). In addition, landslides can evolve into rapidly travelling flows, which exhibit characteristics of debris flows on unchannelized or only weakly channelized hillslopes. The geomorphic heterogeneity of rapid shallow landslides, such as hillslope debris flows, is larger than observed in channelized debris flows; however many of these flows can be successfully modelled using the Voellmy-fluid friction (Christen et al., 2012). Results presented in this paper support the conclusion that Voellmy-fluid rheological model can be used to simulate flow-type landslides.

The selection of model parameters remains one of the fundamental challenges for numerical calculations of natural hazards. At present, there are numerous empirical parameters obtained from 30-years of monitoring data. Such as in RAMMS, we can automatically generate the friction coefficient of an avalanche for our calculation domain based on topographic data analysis, forest information and global parameters (WSL, 2013). The friction parameters for debris flows can found in some literature (Fannin et al., 2001; Iovine et al., 2003; Hürlimann et al., 2008; Scheidl et al., 2010; Huang et al., 2015). However, there is little research regarding friction parameters of flow-type landslide. Therefore, we tested different coulomb friction coefficient μ values ranging between $0.1 \leq \mu \leq 0.6$ and viscous friction coefficient ζ values ranging between $100 \leq \mu \leq 1000 m \cdot s^{-2}$. Finally, we selected the coulomb friction coefficient $\mu = 0.45$ and viscous friction coefficient $\zeta = 500 m \cdot s^{-2}$ in accordance with back-analyses of well-documented landslides (Cepeda et al., 2010; Du et al., 2015). Simulation results are consistent with field observations of topography and sliding path.

Based on the finite volume method and program RAMMS, ~~the~~ simulation results of Taziping landslide were consistent with the sliding path predicted by the field investigation. This correlation indicates that numerical simulation is an effective method for studying the movement processes of flow-type landslide~~s~~ ~~debris flows~~. The accumulation ~~thickness~~ flow height and pressure of landslide deposits were reduced by about 1/2, and the kinematic speed was reduced by about 1/3 after treatment. However, the Miaoba residential area of Red Village is still partially at hazard. Considering that two-story and lower houses within the deposition range might be buried, it was further suggested that the design strength of the gable walls of houses on the middle and upper parts of the deposit be increased above 150kPa.

By utilizing a GIS platform in combination with landslide hazard assessment indexes, we mapped the ~~3~~2D division of the Taziping landslide hazard zones before and after engineering treatment. The results indicated that overall hazard zones contracted after engineering treatment and, the area of high-hazard zones was reduced by about 2/3. After engineering treatment, the number of at hazard houses on the left

[a17]: Answer to the comment Q3 : This paper adopted the RAMMS to simulate the mass movement process. In RAMMS, we can automatically generate the friction coefficient for our calculation domain based on topographic data analysis, forest information and global parameters and so on. Therefore, we can use a changed frictional resistance. This problem has considered in the discussion section.

23

side of the upper Miaoba residential area, was reduced from eight to four. It was thus clear that some zones are still at high hazard despite engineering treatment. Therefore, it was proposed that houses located in high-hazard zones be relocated or reinforced for protection.

Reference

Bartelt, P., Bühler, Y., Buser, O., Christen, M., and Meier, L.: Modeling massdependent flow regime transitions to predict the stopping and depositional behavior of snow avalanches, J. Geophys. Res., 117, F01015, doi:10.1029/2010JF001957, 2012 .

Costa, J.E.: Physical geomorphology of debris flows. Developments and Applications of Geomorphology, Springer Press., 268-317, 1984.

Christen, M., Kowalski, J., and Bartelt, P.: RAMMS: Numerical simulation of dense snow avalanches in three-dimensional terrain, Cold Regions Science and Technology., 63, 1–14, 2010.

Christen, M., Bartelt, P., and Kowalski, J.: Back calculation of the In den Arelen avalanche with RAMMS: interpretation of model results, Annals of Glaciology., 51, 161–168, 2010.

Christen, M., Bühler, Y., Bartelt, P., Leine, R., Glover, J., Schweizer, A., Graf, C., McArdell, B., Gerber, W., Deubelbeiss, Y., Feistl, T., and Volkwein, A.: Integral hazard management using a unified software environment: numerical simulation tool "RAMMS" for gravitational natural hazards, In: Koboltschnig, G., Hübl, J., Braun, J. (eds.) Proceedings of 12th Congress INTERPRAE., 1, 77–86, 2012.

Chen, J.C., and Chuang, M.R.: Discharge of landslide-induced debris flows: case studies of Typhoon Morakot in southern Taiwan, Nat. Hazards Earth Syst. Sci., 14, 1719-1730, 2014.

Cepeda, J., Chávez, J.A., and Martínez, C.C.: Procedure for the selection of runout model parameters from landslide back-analyses：application to the Metropolitan Area of San Salvador, El Salvador, Landslides., 7, 105–116, 2010.

Du, J., Yin, K.L., and Wang, J.J.: Simulation of three-dimensional movement of landslide-debris flow based on finite volume method, Chinese Journal of Rock Mechanics and Engineering., 34: 480–488, 2015 (in Chinese).

[a18]: Answer to the comment Q7 : We have revised all references and quotations in the manuscript according to the NHESSD journal style. The reference list has been updated as well.

24

470 Evans, S.G., Tutubalina, O.V., Drobyshev, V.N., Chernomorets, S.S., McDougall, S., Petrakov,
471   D.A., and Hungr, O.: Catastrophic detachment and high-velocity long-runout flow of Kolka
472   Glacier, Caucasus Mountains, Russia in 2002, Geomorphology., 105, 314–321, 2009.
473 Fannin, R.J., and Wise, M.P.: An empirical-statistical model for debris flow travel distance,
474   Canadian Geotechnical Journal., 38, 982–994, 2001.
475 Finlay, P.J., Mostyn, G.R., and Fell, R.: Landslide risk assessment: prediction of travel distance,
476   Canadian Geotechnical Journal., 36, 556–562, 1999.
477 Fell, R., Corominas, J., Bonnard, C., Cascini, L., Leroi, E., and Savage, W. Z.: Guidelines for
478   landslide susceptibility, hazard and risk zoning for land use planning, Engineering Geology.,
479   102, 85–98, 2008.
480 Fannin, R., and Wise, M.: An empirical-statistical model for debris flow travel distance, Can
481   Geotech J ., 38, 982–994, 2001.
482 Glade, T.: Linking debris-flow hazard assessments with geomorphology. Geomorphology., 66(1):
483   189-213, 2005.
484 Glade, T., Anderson, M. G., Crozier, M.J.: Landslide hazard and risk. Wiley., 75-138, 2006.
485 GB 50010–2010.: Code for design concrete structures, Beijing: Chinese Architectural Industry.,
486   34–80, 2010 (in Chinese).
487 Hebei Province Institute of Hydrogeological and Engineering.: Geological investigation
488   engineering supplemental survey report of Hongse Village Taziping landslide in Hongkou
489   Town of Dujiangyan City, Sichuan Province., 2010 (in Chinese).
490 Hungr, O.: A Model for the runout analysis of rapid flow slides, debris flows and avalanches, Can
491   Geotech J ., 32, 610–623, 1995.
492 Hungr, O., Evans, S.G., Bovis, M,J., and Hutchinson, J,N.: A review of the classification of
493   landslides of the flow type, Environ Eng Geosci., 7, 221–238, 2001.
494 Hungr, O., Morgan G.C., and Kellerhals, R.: Quantitative analysis of debris torrent hazards for
495   design of remedial measures, Can Geotech J., 21, 663–677, 1984.
496 Hu, K.H., Cui, P., and Zhang, J.Q., Characteristics of damage to buildings by debris flows on 7
497   August 2010 in Zhouqu, Western China, Nat Hazards Earth Syst Sci., 12, 2209–2217, 2012.
498 Hürlimann, M., Rickenmann, D., Medina, V., and Bateman, A.: Evaluation of approaches to
499   calculate debris-flow parameters for hazard assessment, Eng Geol., 102, 152–163, 2008.
500 Huang, Y., Cheng, H., Dai, Z., Xu, Q., Liu, F., Sawada, K., Moriguchi, S., and Yashima, A.:
501   SPH-based numerical simulation of catastrophic debris flows after the 2008 Wenchuan
502   earthquake, Bull Eng Geol Environ., 74, 1137–1151, 2015.
503 Iverson, R. M., Reid, M. E., and LaHusen, R. G.: Debris-flow mobilization from landslides, Annu.
504   Rev. Earth Planet Sc., 25, 85– 138, 1997.
505 Iverson, R.M., and Vallance, J.W.: New views of granular mass flows, Geology., 29, 1115–1118,
506   2001.
507 Iovine, G., Gregorio, S,D., and Lupiano, V.: Debris-flow susceptibility assessment through cellular
508   automata modeling: an example from 15–16 December 1999 disaster at Cervinara and San
509   Martino Valle Caudina (Campania, southern Italy), Nat Hazards Earth Syst Sci., 3, 457–468,
510   2003.
511 Jackson, L.E., Kostashuk, R.A., and MacDonald, G.M.: Identification of debris flow hazard on
512   alluvial fans in the Canadian Rocky mountains, Geological Society of America., 7, 155–124,
513   1987.

LeVeque, R.: Finite Volume Methods for Hyperbolic Problems, Cambridge Texts in Applied Mathematics Cambridge University Press., 2002.

~~Michael,L.M., 2003. Baynes F, Scott G, Granger K Regional landsliderisk to the Cairns community[J]. NatHazards, 2003,30 (2):233–249.~~

Michael-Leiba, M., Baynes, F., Scott, G., and Granger, K.: Regional landsliderisk to the Cairns community, NatHazards., 30, 233–249, 2003.

Morgenstern, N.R., and Price, V.E.: The analysis of the stability of general slip surfaces, Geotechnique., 15, 79–93, 1965.

Portilla, M., Chevalier, G., and Hürlimann, M.: Description and analysis of the debris flows occurred during 2008 in the Eastern Pyrenees, Nat. Hazards Earth Syst. Sci., 10, 1635–1645, 2010.

Petrazzuoli, S,M., and Zuccaro, G.: Structural resistance of reinforced concrete buildings under pyroclastic flows: a study of the Vesuvian area, J Volcanol Geoth Res., 133, 353–367, 2004.

Sassa, K., Nagai, S., Solidum, R., Yamazaki, Y., and Ohta, H.: An integrated model simulating the initiation and motion of earthquake and rain induced rapid landslides and its application to the 2006 Leyte landslide, Landslides., 7, 219–236, 2010.

Scott, K.M., and Vallance, J.W.: History of Landslides and Debris Flows at Mount Rainier: Water Fact Sheet, USGS Open-File Report., 93–111, 1993.

Shi,G.H.: Discontinuous deformation analysis - a new numerical model for the statics and dynamics of block system, Berkeley: University of California., 1988.

DZ/T 0286-2015.: Specification of risk assessment for geological hazard, Ministry of Land and Resources of the People's Republic of China., 2015 (in Chinese).

Scheidl, C., and Rickenmann, D.: Empirical prediction of debris-flow mobility and deposition on fans, Earth Surf Proc Land., 35, 157–173, 2010.

Toro, E.F.: Riemann problems and the waf method for solving the two dimensional shallow water equations. Philos. Trans. R. Soc. London., Ser. A 338, 43–68, 1992.

Varnes, D.J., : Slope movement types and processes. In: Schuster RL, Krizek RJ (eds) Landslides: analysis and control. Transportation Research Board, National Research Council, Washington, DC, USA., 11–33 , 1978.

Wang, L., Li, B., Gao, Y., and Zhu, S.: Run-out prediction of large thick-bedded unstable rock: A case study of Daxiang unstable rock in Yangjiao town, Wulong county, Chongqing, Earth Science Frontiers., 23, 251–259, 2016 (in Chinese).

WSL.: RAMMS: A numerical model for snow avalanches in research and practice, User manual v1.5 avalanche, WSL Institute for snow and avalanche research SLF, Swiss., 2013.

~~Yin, K.L., Jiang, Q.H., and Wang, Y.: Simulation of Landslide Movement Process by Discontinuous Deformation Analysis, Earth Science Journal of China University of Geosciences, 27, 632–636, 2002 (in Chinese).~~

~~Zhang, Y.J.: Study on dynamic characteristics of typic rock avalanche on canyon area, Shanghai Jiao Tong University, 2013 (in Chinese).~~

~~Zhang, Z.Y., Wang, S.T., Wang, L.S., Huang, R.Q., Xu, Q., and Tao, L.J.: Principles of engineering geology, Beijing：Geology Press., 212-224, 1993 (in Chinese).~~

Zeng, C., Cui, P., Su, Z.M., Lei, Y., Chen, R.: Failure modes of reinforced concrete columns of buildings under debris flow impact, Landslides., 12, 561-571, 2015.

MogoEdit

CERTIFICATE OF ENGLISH EDITING

This is to certify that the manuscript entitled

Hazard Assessment Comparison of the Tazhiping Landslide Before and After Treatment using the finite volume method

commissioned to us has been carefully edited by a native English-speaking editor of MogoEdit, and the grammar, spelling, and punctuation have been verified and corrected where needed. Based on this review, we believe that the language in this paper meets academic journal requirements. Please contact us with any questions.

Gang Zhang

Dr. Gang Zhang
Founder & CEO of MogoEdit

Date of Issue
June 20, 2017

MogoEdit is a professional English editing company who provides English language editing, translation, and publication support services to individuals and corporate customers worldwide. As a company invested by the affiliate fund of Chinese Academy of Science, MogoEdit is one of the leading language editing service providers in China, whose clients come from more than 1000 universities and research institutes.
MogoEdit Website: http://en.mogoedit.com/
500+ native English editors: http://en.mogoedit.com/editors

Mogo
make the world flatter